Naphthoquinone Functionalized Chiral and Achiral 2^0 Amines: Synthesis, Characterization, *In-silico* study

Abstract

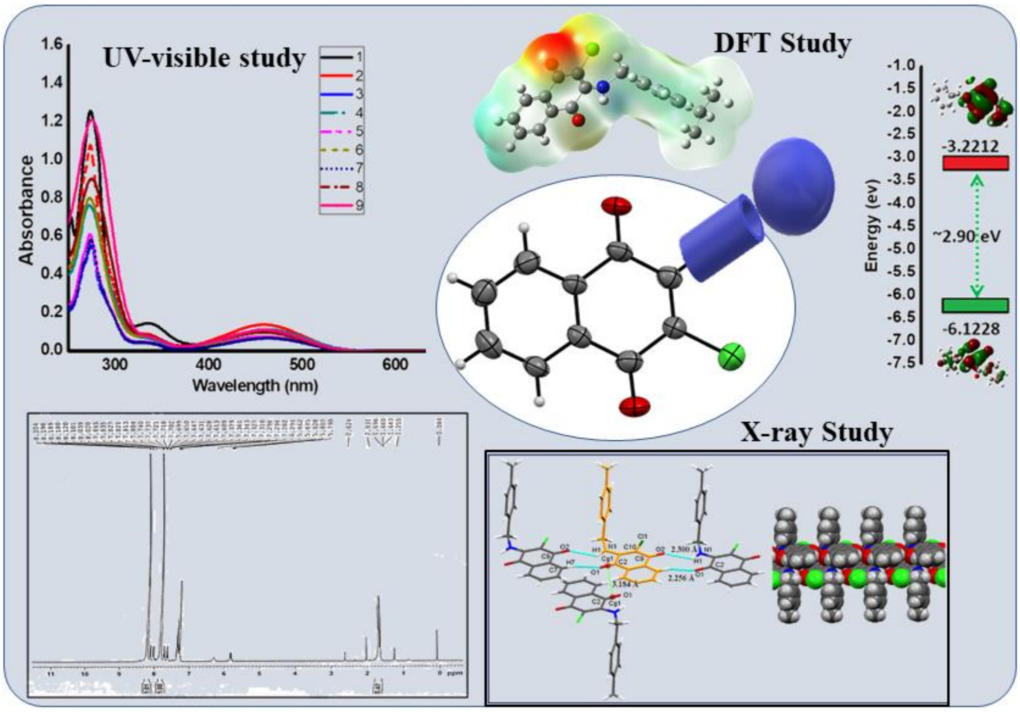

2, 3-dichloro-1,4-naphthoquinone is selected as a lead compound to derive a new series of chiral/ achiral secondary amine ligands such as (R)-2-((1-phenylethyl)amino)-3-chloro-1,4-naphthoquinone (**1**), (S)-2-((1-phenylethyl)amino)-3-chloro-1,4-naphthoquinone (**2**), 2-(4-isopropylbenzylamino)-3-chloro-1,4-naphthoquinone (**3**), 2-((4-methylbenzyl)amino)-3-chloro-1,4-naphthoquinone (**4**), 2-((4-chlorobenzyl)amino)-3-chloro-1,4-naphthoquinone (**5**), 2-((4-fluorobenzyl)amino)-3-chloro-1,4-naphthoquinone (**6**), 2-((4-methoxybenzyl)amino)-3-chloro-1,4-naphthoquinone (**7**), (R)-2-((1-(naphthalen-1-yl)ethyl)amino)-3-chloro-1,4-naphthoquinone (**8**), (S)-2-((1-(naphthalen-1-yl)ethyl)amino)-3-chloro-1,4-naphthoquinone (**9**) under a facile reaction condition in good yield. All the compounds **1-9** were characterized by microanalysis and standard spectroscopic methods such as IR, ^{1}H and ^{13}C NMR and UV-visible absorption spectroscopy. UV-visible absorption spectrum of **1-9** gave a low intensity band at ~450 nm corresponding to charge transfer transitions, a characteristic feature of attached napthoquinone moiety. Notably, compounds exhibit medium to strong fluorescence emission bands in the visible region with concomitant Stokes shifts of ≈ 280 nm.

Supramolecular structures of **1**, **4**, **8** and **9** have been studied by means of single-crystal X-ray diffraction to determine the influence of N-alkyl substituents and chirality on the association of molecules in the solid state. Interestingly, presence of chirality at *N*-alkyl substituent in the compound **1**, successfully switched on C-Cl...O contacts which rather absent in the crystal packing of analogous compound **4**. Analogous compounds **1** and **4** adopt diverse packing patterns forming a fascinating infinite 3D network displaying voids of varied shapes and double sided infinite 1D comb like architecture, respectively. Off more interesting, presence of N-alkyl substituent holding bulker naphthyl groups in **8** and **9** vanished halogen-/ hydrogen bonding contacts seen in the crystal packing of **1** and **4** and that the molecules of **8** and **9** open new strategy of molecular packing by involving vast number of C-H…pi , C-Cl… π, π ... π, C-H…O interactions leading to 3D supramolecular assembly displaying the formation of a number of 3D rectangular /triangular voids. The in-silico study of **1-9** was performed to reinforce the experimental data and to observe the influence of various N-alkyl substituents and chirality on the Protein-ligand interactions with ATPase domain of Topoisomerase-II (PDB:1ZXM).

7.1 Introduction

Interest has been continued on the functionalization of quinones due to their fascinating biological properties.[1] The biological activity of quinone derivatives is reportedly associated with two main properties. First, they are highly redox-active molecules and able to generate reactive oxidative species (ROS), and second, many of them can undergo nucleophilic attack due to their electrophilic character required to facilitate their binding to proteins, DNA, and other biological molecules.[2] They are widely distributed in nature and can be found in the living organisms that include bacteria, fungi, plants and animals. Their important role in the biological processes includes photosynthesis, anti-oxidation, and aerobic respiration.[2] Many quinone derivatives such as vitamin K.[3] 1,4-naphthoquinone, [4] thymoquinone (2-isopropyl-5-methyl-1,4-benzoquinone),[5] emodin (1,3,8- trihydroxy-6-methylanthraquinone),[6] lapachol (2-hydroxy-3-(3-methyl-2-butenyl)-1,4- naphthoquinone),[7] plumbagin (5-hydroxy-2-methyl-1,4- naphthoquinone),[8] juglone (5-hydroxy-1,4-naphthoquinone),[9] and shikonin (5,8-dihydroxy-2-(1-hydroxy-4-methyl-3- pentenyl)-1,4-naphthoquinone),[10] have been shown to exhibit anti-inflammatory and anticancerous activity. Thus, quinone derivatives have a great impact on the biological systems.[11] In particular, the 1,4-naphthoquinone structure is common in numerous natural products associated with antifungal, antibacterial, antiviral and antitumour activities.[12] Very recently, Professor Walhan Alshaer and his research group have shown the ability of 1,4-Naphthoquinone as a potent inhibitor of IRAK1 Kinases.[3c] They have reported a group of quinone derived compounds and systematically examined for their in vitro potential inhibitory effect against human IRAK1 and IRAK4 kinases. They have identified five quinone derived compounds such as 1,4-naphthoquinone, emodin, shikonin, plumbagin, and menadione (vitamin K3) as an active and selective inhibitor of human IRAK1 enzyme. Largely, biological activity of quinonoid systems is connected to their ability to produce free radicals and to facilitate electron transfer to another species in vivo. A variety of biological activities such as antibacterial and antifungal,[13] antiviral, [14] antimalarial,[15] and anticancer,[16] are shown by the derivatives of quinone and thus stimulated their applications as bioactive compounds in the field of medicinal chemistry. Moreover, Professor, Min-Ho Kim *etal* have reported a number of Naphthoquinone-derivative to overcome the antibiotic resistance of methicillin-resistant S. aureus.[17] They have identified lawsone-derivative that exhibited substantial improved drug resistance profiles against MRSA compared to conventional antibiotics. The therapeutic efficacy of the lawsone-derivative was authenticated by using murine models of wound infection as well as non-lethal systemic infection induced by MRSA. It is established that two ketone groups of 1,4-Naphthoquinones act as vital chromophores that can donate or accept electrons in a number of biological systems. In recent studies, the inhibitory mechanism of 1,4- Naphthoquinone derivatives are well-established for irreversible complexation during ROS generation in proteins, leading to loss of protein function.[18] Besides, the hydrogen bonding and stacking interactions involving C–H…O, N–H…O, C–H…π and π…π contacts[19] were considered as main directing tool in the association of molecules in chemistry as well as in biology. However, the recognition of halogen bonding C-H...Cl,[7b, 14, 20] C-Cl…π [8,1521] and C-Cl…O [22] have also been surfaced as another type of directing tool for the association of molecules.[19] They are found to be accountable for the development of a diverse supramolecular assemblies in crystals, biological systems, solutions as well as in the gas phase. A competition between hydrogen bonding and halogen bonding has been observed by the investigators, [19, 23] during supramolecular assembling of organic molecules.

Interestingly, rational modifications of the hierarchy of intermolecular interactions in molecular crystal structures by using switchable halogen bonds were developed.[19, 24] In this chapter, we have demonstrated a facile synthesis of a new series of chiral/ achiral secondary amines such as (R)-2-((1-phenylethyl)amino)-3-chloro-1,4-naphthoquinone (**1**), (S)-2-((1-phenylethyl)amino)-3-chloro-1,4-naphthoquinone (**2**), 2-(4-isopropylbenzylamino)-3-chloro-1,4-naphthoquinone (**3**), 2-((4-methylbenzyl)amino)-3-chloro-1,4-naphthoquinone (**4**), 2-((4-chlorobenzyl)amino)-3-chloro-1,4-naphthoquinone (**5**), 2-((4-fluorobenzyl)amino)-3-chloro-1,4-naphthoquinone (**6**), 2-((4-methoxybenzyl)amino)-3-chloro-1,4-naphthoquinone (**7**), (R)-2-((1-(naphthalen-1-yl)ethyl)amino)-3-chloro-1,4-naphthoquinone (**8**), (S)-2-((1-(naphthalen-1-yl)ethyl)amino)-3-chloro-1,4-naphthoquinone (**9**) from 3, 4-dichloro-1,4-naphthoquinone (**Chart 1**). All the molecules are characterized by microanalysis, NMR (1H and 13C), IR, UV-visible, Fluorescence spectroscopies. Single crystal X-ray diffraction (SCXRD) was used to elucidate the propensity of the molecules of **1**, **4**, **8** and **9** for the formation of diverse supramolecular assembly involving switchable weak intermolecular interactions by scaffold substitutions. Further, in silico study was performed to reinforce the experimental outcomes. The molecular docking study was performed to probe the ability of synthesized compounds in offering secondary interactions of with the active sites of ATPase domain of Topoisomerase-II (PDB:1ZXM) protein and to project their potential biological applicability.

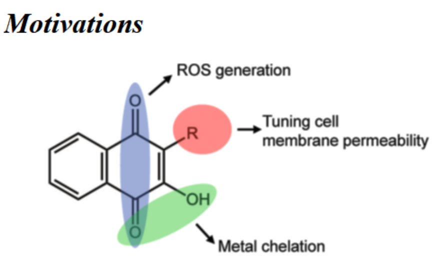

Ronghui Song *et.al.* Commun Biol **3**, 529 (2020).

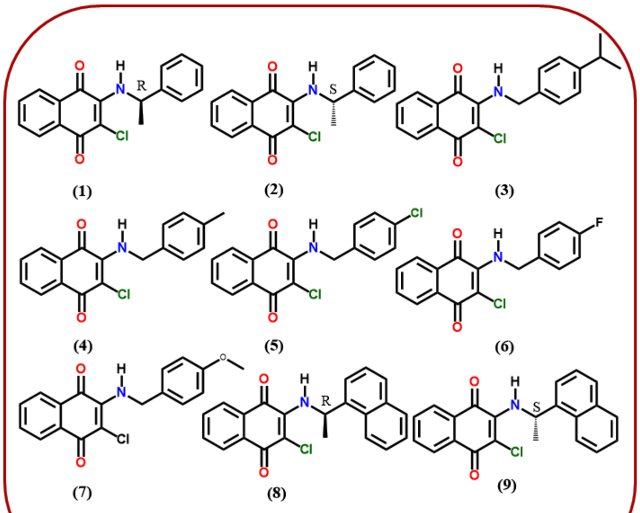

Chart 1: New series of compounds 1-9 under investigation

Chart 1: Compounds **1–9** under investigation.

7.2 Experimental

7.2.1 Materials and measurements

All solvents were purchased from the commercial sources and were freshly distilled prior to use. All the reagents such as 2,3-dichloro-1,4-napthaquinone, (R)-1-phenylethan-1-amine, (S)-1-phenylethan-1-amine, (4-isopropylphenyl)methanamine, 4-methyl benzylamine, (4-chlorophenyl)methanamine, (4-florophenyl)methanamine, (4-methoxyphenyl)methanamine, (R)-1-(naphthalen-1-yl)ethan-1-amine and (S)-1-(naphthalen-1-yl)ethan-1-amine) were purchased from TCI and Sigma-Aldrich Chemicals Limited, these were used without further purification. Elemental analyses (C, H, N) were carried out on a Perkin-Elmer 2400 analysers. Thin Layer Chromatography was performed on Merck 60 F254 Aluminium coated plates. FT-IR spectra were recorded in the 4000-400 cm^{-1} range using a Perkin-Elmer FT-IR spectrometer as KBr pellets. The ^{1}H and ^{13}C NMR spectra of relevant compounds were obtained on a Bruker AV-III 400 MHz spectrometer in spectrometer with $CDCl_3$ as solvent and TMS as internal standard. UV-visible spectra were recorded on a JASCO V-730 UV-visible spectrophotometer. Fluorescence spectra were recorded on a JASCO FP-8200 Fluorescence spectrofluorometer.

7.2.2 General procedure for synthesis of 2-(arylamino)-3-chloro-1,4-naphthoquinones (1-9)

One equivalent of 2,3-dichloro-1,4-napthaquinone (0.5g, 2.202 mmol) was added into a solution containing corresponding amines *viz*. ((R)-1-phenylethan-1-amine (283 µL, 2.202 mmol, d=0.94g/ml), (S)-1-phenylethan-1-amine (283 µL, 2.202 mmol, d=0.94g/ml), (4-isopropylphenyl)methanamine (370 µL, 2.202 mmol, d=0.89g/ml), 4-methyl benzylamine (280 µL, 2.202 mmol, d= 0.952 g/ml), (4-chlorophenyl)methanamine (270 µL, 2.202 mmol, d=1.16 g/ml), (4-florophenyl)methanamine (250 µL, 2.202 mmol, d=1.95g/ml), (4-methoxyphenyl)methanamine (290 µL, 2.202 mmol, d=1.05g/ml), (R)-1-(naphthalen-1-yl)ethan-1-amine (350 µL, 2.202 mmol, d=1.067g/ml) or (S)-1-(naphthalen-1-yl)ethan-1-amine(350 µL, 2.202 mmol, d=1.067g/ml)) in 30 mL of absolute ethanol. The reaction mixture was stirred at 40-50 ^{0}C temperature for 5 hours. During these hours, a change in the colour of the reaction mixture was observed from yellow to red. The progress of the reaction was monitored by the TLCs. The reaction mixture was dried under vacuum and the residue was washed several times with saturated Na_2CO_3

solution followed by 3 × 10 mL of distilled water. The red coloured product was finally dried under vacuum and preserved in desiccator for analysis. The experimental data are summarized in Table 1 and Table 2.

Table 1. Micro-, mass- and IR analysis data for compounds **1-9.**

Entry	Molecular Formula	Molecular Weight	Yield (%)	Elemental Analysis % Found (calculated)			IR data (KBr disc) υ_{max}/cm^{-1}
				C	H	N	
1	$C_{18}H_{14}ClNO_2$	312	88	68.53 (68.42)	4.83 (4.78)	4.37 (4.31)	3326 (N-H), 3097(C-H), 1680(C=O), 1587, 1559, 1274, 1138, 822, 708, 639.
2	$C_{18}H_{14}ClNO_2$	312	87	68.56 (68.58)	4.87 (4.80)	4.48 (4.40)	3329(N-H), 3066(C-H), 1671(C=O), 1605 1573, 1500, 1292, 1132, 822, 720, 698.
3	$C_{20}H_{18}ClNO_2$	340	90	70.85 (70.78)	5.79 (5.71)	4.08 (3.98)	3373 (N-H), 3077(C-H), 1679(C=O), 1597, 1563, 1520, 1274, 1333, 1132, 845, 802, 724.
4	$C_{18}H_{14}ClNO_2$	312	88	70.15 (70.01)	4.73 (4.65)	4.47 (4.39)	3295 (N-H), 3110(C-H), 1677(C=O), 1601, 1572, 1512, 1433, 1304, 1260,1136, 1072, 828, 789, 718
5	$C_{17}H_{11}Cl_2NO_2$	332	85	61.95 (61.88)	3.73 (3.65)	4.93 (4.85)	3293 (N-H), 3110(C-H), 1677(C=O), 1601, 1571, 1510, 1432, 1332, 1332,1305, 1259, 1137, 823, 723, 721.
6	$C_{17}H_{11}ClFNO_2$	316	87	65.09 (65.01)	3.51 (3.45)	4.25 (4.18)	3382 (N-H), 3108(C-H), 1681(C=O), 1600, 1568, 1510, 1443, 1333, 1303, 1256, 1136, 834, 722, 679, 575.
7	$C_{18}H_{14}ClNO_3$	327	86	64.59 (64.48)	4.63 (4.57)	4.72 (4.65)	3281(N-H), 3108(C-H), 1681(C=O), 1599, 1568, 1510, 1460, 1441, 1332, 1303, 1257, 1136, 1030, 835, 722, 586.
8	$C_{22}H_{16}ClNO_2$	362	85	73.67 (73.58)	4.71 (4.65)	4.11 (4.01)	3338 (N-H), 2963(C-H), 1670(C=O), 1640, 1599, 1570, 1492, 1333, 1288, 1139, 805, 781, 721, 738.
9	$C_{22}H_{16}ClNO_2$	362	84	73.74 (73.65)	4.78 (4.69)	4.29 (4.18)	3338 (N-H), 3051(C-H), 1669(C=O), 1599, 1570, 1492, 1333, 1288, 1139, 739, 721.

Table 2. NMR spectral data for compounds **1-9.**

Entry	**NMR Data (ppm)**	
	^{1}H NMR ($CDCl_3$)	**^{13}C NMR ($CDCl_3$)**
1	8.15 (dd, *J* = 7.2 Hz, 2H, -quinone), 7.68 (d, *J* = 7.2 Hz, 2H, -quinone), 7.28-7.37 (m, 5H, -Ph), 6.29 (s, 1H; NH), 5.83 (m, 1H, CH), 1.66 (d, 3H, CH_3).	180.0, 176.0, 143.8, 134.9, 132.7, 130.9,128.9, 127.6, 126.9, 125.6, 53.36, 24.65
2	8.10 (dd, *J* = 7.2 Hz, 2H, -quinone), 7.69 (d, 2H, *J* = 7.2 Hz, -quinone), 7.28-7.38 (m, 5H, -Ph), 6.30 (s, 1H; NH), 5.81 (m, 1H, CH), 1.64 (d, 3H, CH_3).	180.4, 176.9, 143.8, 134.9, 132.5, 128.9, 127.6, 126.8, 125.7, 111.6, 53.36, 24.65
3	8.13 (dd, *J* = 7.2 Hz, 2H, -quinone), 8.02 (d, *J* = 7.2 Hz, 2H, -quinone), 7.70 (dd, 2H, -Ph), 7.61 (dd, 2H, -Ph), 5.96 (s, 1H; NH), 4.80 (m, 1H, CH), 1.32 (d, 6H, CH_3).	180.5, 176.9, 143.3, 134.9, 132.7, 129.6, 126.8, 45.74, 24.34
4	8.08 (dd, 2H, -quinone), 8.02 (d, 2H, -quinone), 7.18-7.28 (m, 4H, -Ph), 6.22 (s, 1H; NH), 5.01 (d, 2H, CH_2), 2.36 (s, 3H, CH_3).	180.3, 176.9, 144.0, 137.8, 134.9, 132.62, 129.71, 127.7, 126.8, 48.7, 21.19
5	8.14 (dd, 2H, -quinone), 8.10 (d, 2H, -quinone), 7.35 (d, 2H, -Ph), 7.28 (d, 2H, -Ph), 6.25 (s, 1H; NH), 5.02 (d, 2H, CH_2).	180.3, 176.9, 143.8, 136, 135.0, 133.8, 132.6, 129.7, 128.9, 126.9
6	8.12 (dd, 2H, -quinone), 8.03 (d, 2H, -quinone), 7.62 (d, 2H, -Ph), 7.29 (d, 2H, -Ph), 6.22 (s, 1H; NH), 5.02 (d, 2H, CH_2).	180.3, 176.9, 176.0, 163.6, 161.1, 143.8, 135.0, 133.7, 132.6, 130.8, 129.6, 127.8, 111.34, 48.1
7	8.13 (dd, 2H, -quinone), 8.05 (d, 2H, -quinone), 7.73 (d, 2H, -Ph), 7.65 (d, 2H, -Ph), 6.41 (s, 1H; NH), 4.98(d, 2H, CH_2), 3.82(s, 3H, OCH_3).	180.3, 176.9, 159.4, 143.9, 134.9, 132.6, 129.7, 126.8, 114.3, 55.34, 48.5
8	8.15 (dd, 2H, -quinone), 8.08 (d, 2H, --quinone), 7.45-7.65 (m, 7H, -Naph), 6.65 (m, 1H, CH), 6.41 (s, 1H; NH), 1.80 (d, 3H, CH_3).	180.4, 176.9, 143.0, 139.1, 134.9, 132.5, 130.2, 129.7, 128.4, 126.9, 125.8, 122.7, 49.6, 23.5
9	8.16 (dd, 2H, -quinone), 8.09 (d, 2H, --quinone), 7.46-7.75 (m, 7H, -Naph), 6.64 (m, 1H, CH), 6.41 (s, 1H; NH), 1.80 (d, 3H, CH_3).	180.4, 176.9, 139.1, 134.9, 132.0, 130.2, 129.7, 128.4, 127.8, 126.9, 125.8, 122.7, 49.6, 23.5

7.2.3 X-ray crystallography and data collection

Crystals of **1, 4, 8** and **9** suitable for X-ray crystallographic study were obtained in ethylacetate solution by slow evaporation at 4 °C. The intensity data were collected on Oxford diffraction X Calibur diffractometer equipped with Eos CCD detector at 293 K for [$C_{18}H_{14}ClNO_2$] **1**, [$C_{18}H_{14}ClNO_2$] **4**, [$C_{22}H_{16}ClNO_2$] **8** and [$C_{22}H_{16}ClNO_2$] **9** respectively. Monochromatic Mo-*Kα* X-ray (λ=0.71073 Å) was used for the measurements. Data were collected and reduced by using the ‘‘CrysAlispro’’ program.[25] An empirical absorption correction using spherical harmonics was implemented in ‘‘SCALE3 ABSPACK’’ scaling algorithm. The crystal structures were solved by direct methods using SHELXL-97 [26] and the refinement was carried out against F^2 using SHELXL-97 program package.[27] All non-hydrogen atoms were refined anisotropically.

7.2.4 Molecular Docking

Ligand preparation:

The designed ligands were sketched using Chem Draw 19.0 and the molecules were converted into 3D in ChemBio 3D. The sketched molecules were converted into .mol format using Open Babel Graphical User Interface (OBGUI) software.[28] Molecules in mol format were retrieved into Biovia Discovery Studio’s Client 20 and the ligands were minimized using fast deriding like force field.

Protein Preparation:

The proteins with PDB ID: 1ZXM was downloaded from protein data bank and retrieved into the workspace of Discovery Studio Client. The proteins were prepared using protein preparation wizard and the errors in the protein were minimized using preparation protocol. The protein qualities were assigned using hydrophobicity plot and ramachnadran plot.

Grid Preparation:

The proteins active site selected within the 3D co-ordinates of co-crystallized ligand (binding pocket). The ligands were docked onto the active site of protein using autodock 4.0, C-docker of Discovery Studio Client 20.0. The docking protocol was validated by re-docking the co-crystallized ligand onto binding pocket/active site.

Auto Dock 4.0

Docking was performed using rigid docking the auto dock 4.0.[29] All the ligands were screened for their efficient fitting into the receptor (minimized) grid, and all the docking parameters including binding energy were calculated with optimized RMSD. The ligands were screened with 10 possible minimum energy confirmations.

Visualization of residues Interaction

The lead ligands interact with active site either by Hydrogen bonding or by Hydrophobic Interactions. All the post processing was done using Discovery Studios & or with ICM-Pro software of Molsoft.com.

7.3 RESULTS AND DISCUSSION

7.3.1 Synthesis and Characterization

A typical reaction involving primary amine viz (R)-1-phenylethan-1-amine, (S)-1-phenylethan-1-amine, (4-isopropylphenyl)methanamine, 4-methyl benzylamine, (4-chlorophenyl)methanamine, (4-florophenyl)methanamine, (4-methoxyphenyl)methanamine, (R)-1-(naphthalen-1-yl)ethan-1-amine or (S)-1-(naphthalen-1-yl)ethan-1-amine) and 2,3-dichloro-1,4-napthaquinone in absolute EtOH affords access to a new series of chiral /achiral secondary amines (R)-2-((1-phenylethyl)amino)-3-chloro-1,4-naphthoquinone (**1**), (S)-2-((1-phenylethyl)amino)-3-chloro-1,4-naphthoquinone (**2**), 2-(4-isopropylbenzylamino)-3-chloro-1,4-naphthoquinone (**3**), 2-((4-methylbenzyl)amino)-3-chloro-1,4-naphthoquinone (**4**), 2-((4-chlorobenzyl)amino)-3-chloro-1,4-naphthoquinone (**5**), 2-((4-fluorobenzyl)amino)-3-chloro-1,4-naphthoquinone (**6**), 2-((4-methoxybenzyl)amino)-3-chloro-1,4-naphthoquinone (**7**), (R)-2-((1-(naphthalen-1-yl)ethyl)amino)-3-chloro-1,4-naphthoquinone (**8**), (S)-2-((1-(naphthalen-1-yl)ethyl)amino)-3-chloro-1,4-naphthoquinone (**9**) as shown in the Scheme 1. After workup the products were obtained as reddish powder in 84‒90% isolated yields. All the compounds **1-9** have been characterized thoroughly by microanalysis, standard spectroscopy technique. The spectroscopic analysis data, such as IR, NMR and UV-visible spectra of the compounds **1-9** are consistent with their chemical formula determined by elemental analysis. The molecular structures of **1**, **4**, **8** and **9** were further confirmed by single crystal X-ray diffraction study. In the IR spectra of **1-9**, the most characteristic bands observed between 3282– 3373 cm^{-1} are indicative of υ(N-H) stretching vibrations. The aromatic υ(C-H) stretching vibrations are appeared as a weak intensity band in the regions of 3110-2963 cm^{-1} whereas bands appeared in the regions of 845-822 cm^{-1} are assignable to the aromatic υ(C-H) out-of plane bending vibrations, a characteristic feature of phenyl groups in **1-9**.

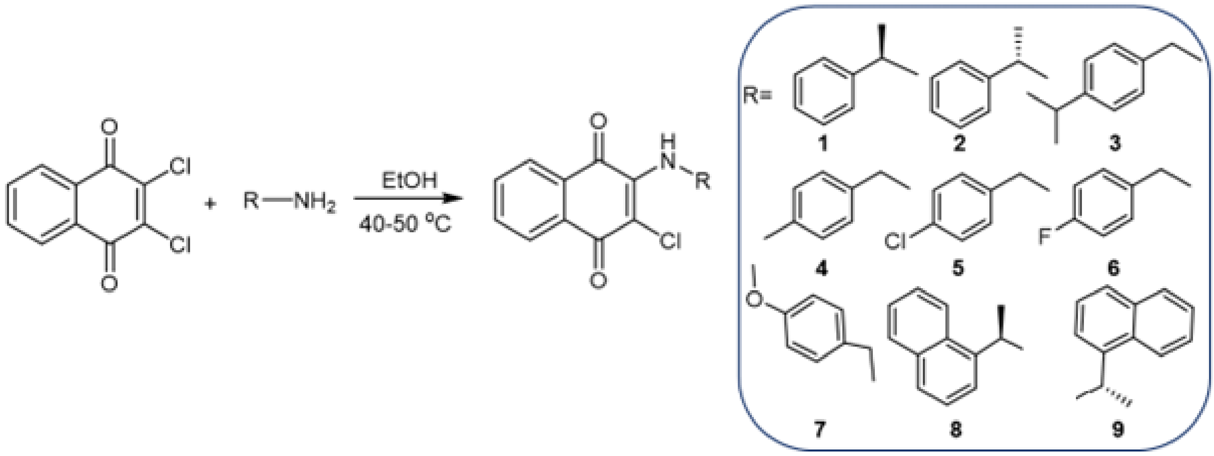

Scheme 1. General synthetic strategies adopted for naphthoquinone derivatives (1-9).

Compounds **1-9** display additional bands in 1681–1669 cm^{-1} and 1139-1132 cm^{-1} region due to υ(C=O) and υ(C-N) vibrations.[19] Compounds **1-9** display a sharp band in the region of 722-708 cm^{-1} due to υ(C-Cl) stretching vibrations (Table 1). The most characteristic ^{1}H NMR signals of 1-9 appeared in the range of δ = 5.96-6.41 ppm (Table 2) due to amine –NH moiety. Besides, ^{1}H NMR signals due to aromatic protons with proper splitting pattern have also the observed. A significant up-field shifting of –NH signal in compound 3 is observed due to presence of electron donating isopropyl aromatic substituent and vice versa. The most characteristic ^{13}C NMR signals of 1-9 appeared in the range of δ = 180–176 ppm due to quinonic carbonyl moieties, apart from the signals due to various aromatic and aliphatic carbons. The IR, ^{1}H and ^{13}C NMR spectral data for **1-9** are consistent with similar compounds reported in the literature.[19]

7.3.2 X-ray crystallographic study

Single crystals for **1**, **4**, **8** and **9** suitable for single crystal X-ray diffraction study, were grown from ethylacetate solution by slow evaporation at 4 °C. The crystal data and structure refinement for compounds **1**, **4**, **8** and **9** are given in Table 3. Compounds crystallize in chiral triclinic *P-1* space group (for **1**), monoclinic C2/c space group (for **4**) and orthorhombic $P2_12_12_1$ space group (for **8** and **9**). The X-ray crystal structure of **1**, **4**, **8** and **9** shows asymmetric unit containing full molecule as shown in Figure 1. There are one and eight such molecules in the unit cell of compounds **1** and **4** respectively, while four such molecules are present in the unit cell of **8** and **9**.

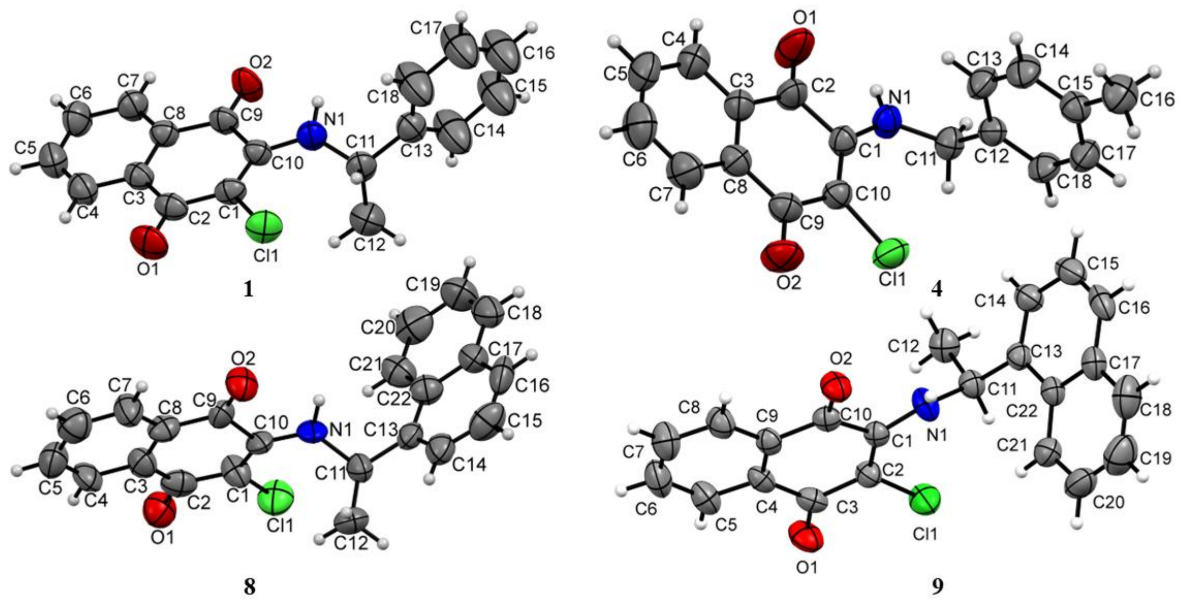

Figure 1. Thermal ellipsoidal plot of **1**, **4**, **8** and **9** with atomic numbering scheme.

The structural parameters such as bond lengths and bond angles (Table 4) are found to be consistent with the literature. [19, 30] Notably, the C-N bonds holding naphthoquinone moieties are significantly shorter than the similar bonds holding alkyl groups in these molecules.

Table 3. Crystal data and structure refinement for the compounds under investigation.

Code	1	4	8	9
Empirical formula	$C_{18}H_{14}ClNO_2$	$C_{18}H_{14}ClNO_2$	$C_{22}H_{16}ClNO_2$	$C_{22}H_{16}ClNO_2$
Formula weight	311.75	311.75	361.81	361.81
Temperature/K	293	293	293	293
Crystal system	triclinic	monoclinic	orthorhombic	orthorhombic
Space group	P1	C2/c	$P2_12_12_1$	$P2_12_12_1$
a/Å	5.2381(3)	26.4512(9)	5.4764(10)	5.4789(8)
b/Å	5.7804(4)	7.6691(2)	12.469(3)	12.492(2)
c/Å	12.5094(6)	15.0381(5)	25.724(7)	25.759(4)
α/°	85.047(5)	90	90	90
β/°	87.858(4)	96.958(3)	90	90
γ/°	83.809(5)	90	90	90
Volume/Å^3	375.00(4)	3028.14(17)	1756.5(7)	1762.9(5)
Z	1	8	4	4
ρ_{calc}g/cm^3	1.38	1.368	1.368	1.363
μ/mm^{-1}	0.261	0.258	0.234	0.233
F(000)	162	1296	752	752
Radiation	Mo Kα (λ = 0.71073)	Mo Kα (λ = 0.71073)	Mo Kα (λ = 0.71073)	Mo Kα (λ = 0.71073)
2Θ range for data collection/°	6.54 to 64.46	5.94 to 64.38	6.72 to 50.8	6.52 to 57.94°
Index ranges	-7 ≤ h ≤ 5, -8 ≤ k ≤ 8, -18 ≤ l ≤ 17	-37 ≤ h ≤ 37, -10 ≤ k ≤ 11, -22 ≤ l ≤ 22	-5 ≤ h ≤ 5, -13 ≤ k ≤ 13, -27 ≤ l ≤ 27	-7 ≤ h ≤ 6, -16 ≤ k ≤ 15, -34 ≤ l ≤ 33
Reflections collected	4095	19056	7686	11477
Independent reflections	2998 [R_{int} = 0.0197, R_{sigma} = 0.0311]	5038 [R_{int} = 0.0387, R_{sigma} = 0.0326]	2248 [R_{int} = 0.1652, R_{sigma} = 0.1980]	4118[R(int) = 0.0751]
Data/restraints/parameters	2998/3/176	5038/0/200	2248/0/236	4118/0/236
Goodness-of-fit on F^2	1.201	1.314	0.907	1.046
Final R indexes [I>=2σ (I)]	R_1 = 0.0571, wR_2 = 0.1737	R_1 = 0.0684, wR_2 = 0.2109	R_1 = 0.0799, wR_2 = 0.1675	R_1 = 0.0637, wR_2 = 0.0920
Final R indexes [all data]	R_1 = 0.0694, wR_2 = 0.1915	R_1 = 0.1090, wR_2 = 0.2423	R_1 = 0.1780, wR_2 = 0.2477	R_1 = 0.1490, wR_2 = 0.1234
Largest diff. peak/hole / e Å^{-3}	0.46/-0.29	0.57/-0.37	0.41/-0.23	0.20/-0.22

Table 4. Selected geometrical parameters obtained from Xray structure **1**, **4**, **8** and **9.**

Entry	Selected Bond	Bond lengths [Å]	Selected Bonds	Bond angles [˚]
1	C11-C13	1.518(5)	C13-C11-C12	113.4(4)
	C11-C12	1.543(7)	C13-C11-N1	108.1(3)
	C11-N1	1.450(4)	C12-C11-N1	109.0(4)
	N1-C10	1.358(5)	N1-C10-C1	130.0(3)
	C1-Cl1	1.731(4)	C10-C1-Cl1	122.2(3)
4	C11-C12	1.518(3)	C12-C11-N1	114.14(17)
	C11-N1	1.450(3)	C11- N1-C1	130.38(19)
	N1-C1	1.347(3)	N1-C1-C10	131.1(2)
	C10-Cl1	1.737(2)	C1-C10-Cl1	122.37(17)
8	C11-C13	1.513(13)	C13-C11-C12	114.7(10)
	C11-C12	1.512(13)	C13-C11-N1	106.2(8)
	C11-N1	1.482(12)	C12-C11-N1	108.5(9)
	N1-C10	1.335(12)	N1-C10-C1	131.2(10)
	C1-Cl1	1.736(10)	C10-C1-Cl1	120.4(9)
9	C11-C13	1.518(4)	C13-C11-C12	115.6(3)
	C11-C12	1.514(4)	C13-C11-N1	107.4(2)
	C11-N1	1.485(4)	C12-C11-N1	108.7(3)
	N1-C1	1.350(4)	N1-C1-C2	128.8(3)
	C2-Cl1	1.725(3)	C1-C2-Cl1	122.2(3)

The single crystal X-ray diffraction data reveals that a change in the chirality and the *N*-substituents, changes the electronic nature as well as stereochemical conformations of the molecules which can be seen from the variations in the dihedral angles between the least squares plane through the naphthoquinone rings and that *N*-substituents. The naphthoquinone moiety having extended conjugation keep both the naphthoquinone rings virtually planar in **1** and **2** however a substantial deviation from coplanarity of naphthoquinone rings is observed in case of compounds **8** and **9**. For instance, the angle between the least squares planes through benzene and quinone rings of naphthoquinones appeared at 1.33° (in case of **1**), 0.64° (in case of **4**), 5.73° (in case of **8**) and 5.44 (in case of **9**). Notably, a '*gauche*' conformational mode of naphthoquinone ring and benzene ring planes in **1** and **4** is revealed by the dihedral angle ~77° calculated from the least squares planes going through the quinone ring and benzene ring of various *N*-substituent, however, a significant deviation of naphthoquinone ring and naphthyl ring planes in **8** and **9** from a stable '*gauche*' conformational mode of is revealed by their dihedral angles ~87°. Apparently, such conformational changes induced by various amine *N*-substituents and chirality in the molecules of **1**, **4**, **8** and **9**, modify the nature of donor-acceptor sites for noncovalent interactions, leading to the formation of diverse supramolecular structures. This creates a possibility for the management and fair tuning of the supramolecular assembly arise due to non-covalent interactions in these molecules.

For instance, compound **1** holding chirality at *N*-alkyl substituent adopts a '*gauche*' conformation, predominantly stabilized *via* very interesting C-Cl...O[31] (C-Cl…O = 3.154 Å) intermolecular interactions involving one of the ketonic oxygen and chlorine. Besides, the molecule present in the asymmetric unit forms a supramolecular unit, consists of five molecules aggregate by involving C-H…π (Cg1: centroid of C6C5C4C7C8C3) weak intermolecular contact (3.346 Å), C-H…Cl (2.812 Å) and C-H…O intermolecular contacts (2.627 Å) as shown in Figure 2 (a). The crystal packing included four intermolecular distances significantly shorter than the sum of the van der Waals radii of the atoms involve. Interestingly, these supramolecular units generate infinite 3D network displaying opening of varied shapes along-axis as shown in Figure 2(b) and Figure 2(c).

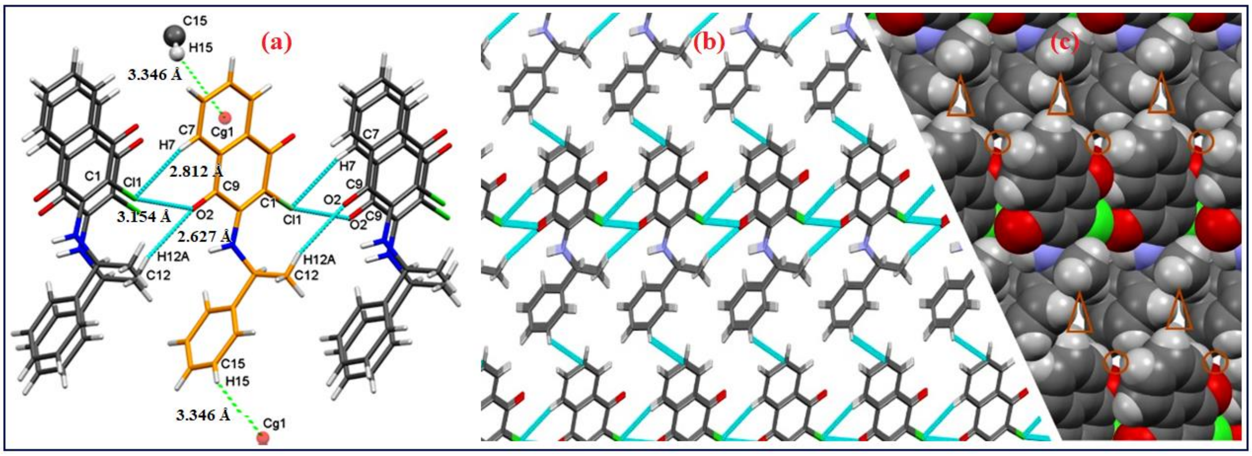

Figure 2. (a) Supramolecular unit consists of five molecule aggregates involving C-Cl...O, C-H…π, C-H…Cl and C-H…O intermolecular interactions by **1**; (b) Capped Sticks and (c) Spacefill representation of molecular packing along *a*-axis (slightly tilted down) displaying 3D opening of varied shapes.

Interestingly, lack of chirality at *N*-alkyl substituent in the analogous compound **4**, successfully switches off C-Cl...O contacts seen in compound **1** and that the new compound adopt other packing patterns based on H-bonding N-H…O (2.300 Å), C-H…O (2.256 Å) and π...π (3.184 Å) intermolecular interactions. Moreover, unlike compound **1**, the *N*-alkyl substituent could not contribute in the supramolecular packing of compound **4.** Further, the molecule present in the asymmetric unit forms a supramolecular unit, consists of four molecules aggregate as shown in Figure 3 (a). Evidently, ketonic carbonyl is involved in the formation of π...π closing contact while N-H…O contacts in cooperation with C-H…O intermolecular contacts extend the dimensionality along b-axis, forming a fascinating 1D double sided comb like structure as shown in the Figure 3 (b) and Figure 3 (c).

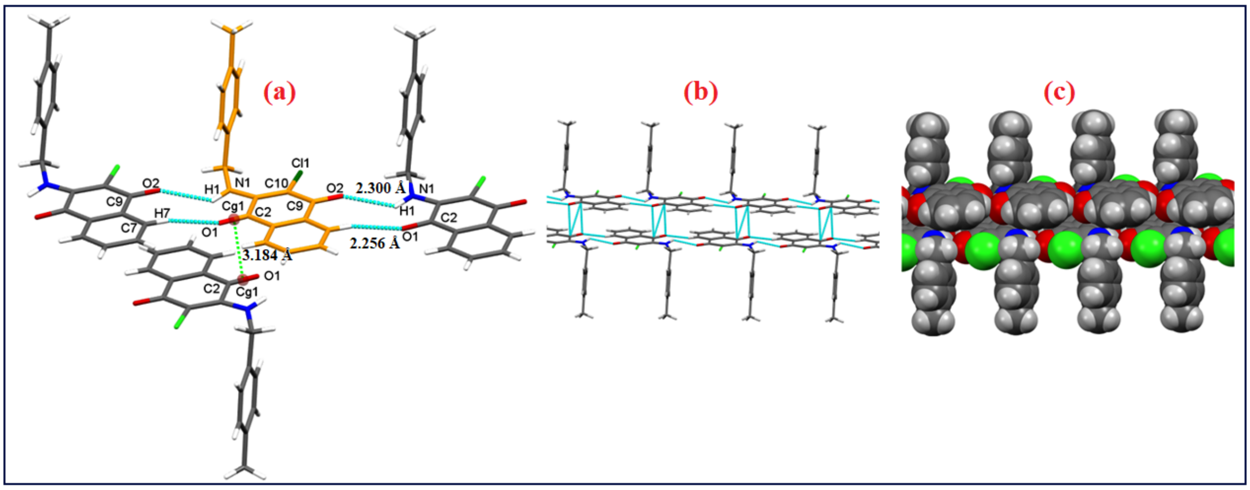

Figure 3. (a) Supramolecular unit consists of four molecule aggregates involving N-H...O, C-H…O, and π...π intermolecular interactions by molecules of **4**; (c) Capped Sticks and Spacefill representation of molecular packing along *a*-axis (slightly tilted down) displaying fascinating double sided comb like architecture.

Off more interesting, presence of N-alkyl substituent holding bulker naphthyl groups in the molecules of **8** and **9** vanished halogen-/ hydrogen bonding interactions seen in the molecular packing of **1** and **4** and that the molecules of **8** and **9** open new strategy of molecular packing by involving vast number of other weak intermolecular forces viz. C-H…pi , C-Cl… π, π ... π, C-H…O as shown in Figure 4 (a) and Figure 4 (b), respectively. The cumulative effect of these interactions resulted into 3D supramolecular assembly displaying the formation of a number of 3D rectangular /triangular voids as shown in the Spacefill model of Figure 5.

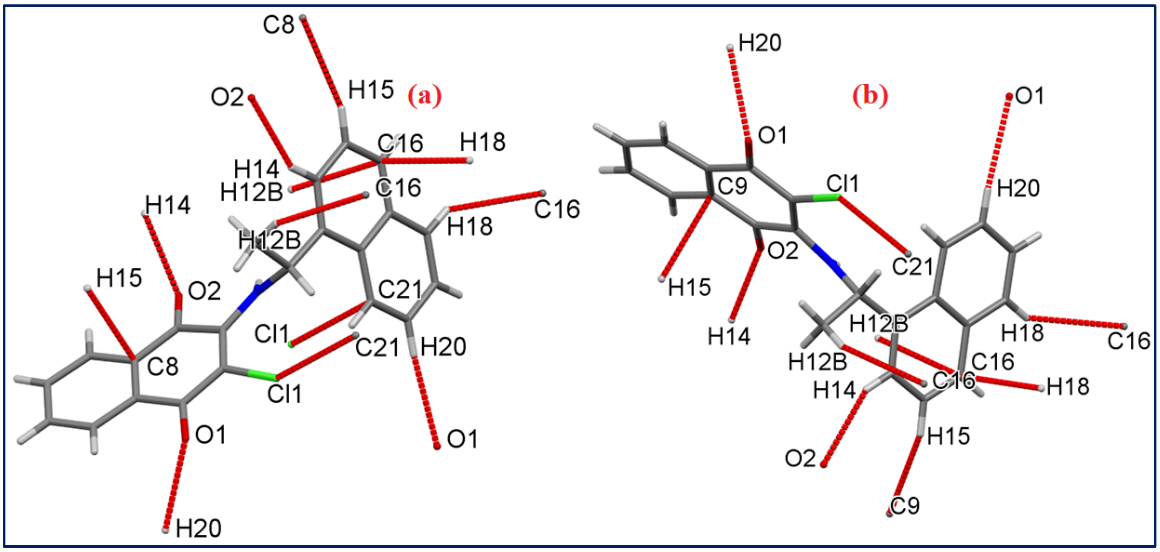

Figure 4. Asymmetric molecule of (a) **8** and (b) **9** opens vast number of weak intermolecular forces viz. C-H…pi , C-Cl… π, π ... π, C-H…O to stabilize the molecules in solid state.

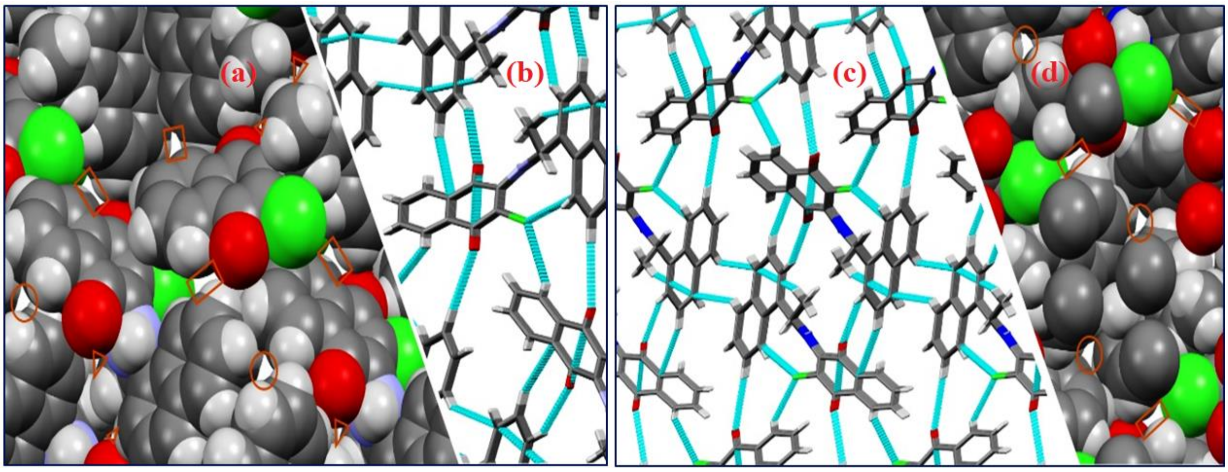

Figure 5. (a) Spacefill model displaying the formation of 3D rectangular and triangular voids by the molecules of 8; (b) & (c) Capped sticks model showing the formation of 3D architecture by the molecules of 8 and 9, respectively; (d) Spacefill model displaying the formation of 3D rectangular and triangular voids by the molecules of 9. All views are along a-axis with slightly downward tilting.

X-ray crystallographic study has helped to understand the ability of these molecules to offer diversified intermolecular molecular interactions which are apparently influenced by chirality/ *N*-alkyl substitutions. These results encouraged us to probe the interplay of secondary interactions of the modified amino nucleus with the ATPase domain of Topoisomerase-II (PDB:1ZXM) protein and to demonstrate the efficacy of these compounds as promising pro-drug (discussed later).

7.3.3 UV-visible absorption and fluorescence properties

The UV-visible absorption (Figure 6) and fluorescence spectral study (Figure 7) of all of the compounds **1-9** have been caried out at room temperature from 10^{-4} M CH_3CN solution and the pertinent results are briefed in Table 5. The assignments were based on the absorption and emission spectra of those of the closely related compounds.[19]

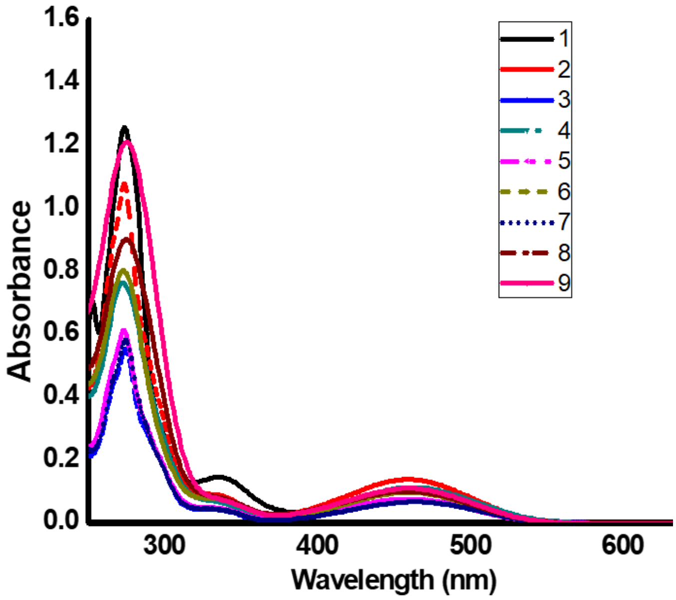

Figure 6. UV-visible absorption spectrum of the compounds under investigation at room temperature in 10^{-4} M CH_3CN.

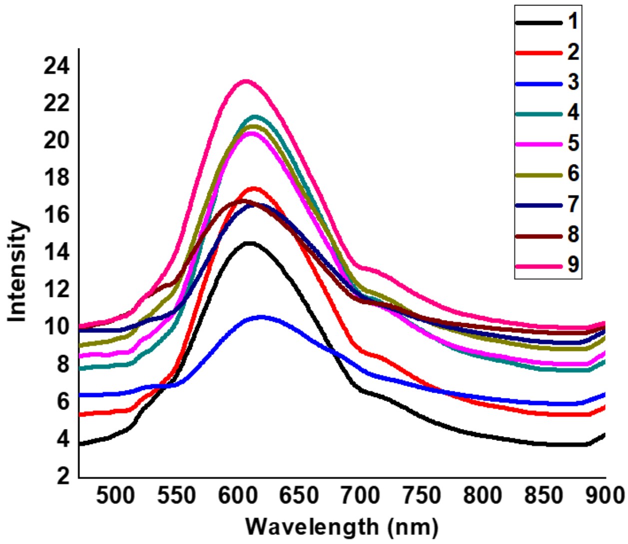

Figure 7. Fluorescence spectrum of the compounds under investigation at room temperature in 10^{-4}M CH_3CN solution.

The UV-visible spectral spectrum of all compounds gives a high intensity absorption band in the region of ~250 nm **(**Figure 6**)** which is mainly attributed to the locally excited π→π* transitions. A broad, low intensity band observed in the ~350 nm region attributable to n→π* and very low intensity band observed in the ~450 nm region attributable to charge transfer transitions, a characteristic feature of attached napthoquinone moiety. Most of the compounds fluoresces in the visible region of upon excitation at 470 nm with a concomitant Stokes shift of ~150 nm. Highest fluorescence intensity was observed for compound **1** holding *N*-1-phenylethyl substituent whereas low intensity band was observed for compound **3** holding *N*-4-isopropylbenzyl substituent.

Table 5. UV-visible and fluorescence bands for compounds under investigation.

Entry	UV-Visible data (10^{-4} CH_3CN) λ_{max} nm (ε L Mol^{-1} cm^{-1})	Fluorescence spectrum data (10^{-4} M CH_3CN)	
		λ_{ex} (nm)	λ_{em} nm (Intensity)
1	273(12529) π→π*, 336 (1497) n→ π*, 461(1059) CT	470	608 (14.5) CT
2	273 (10756) π→π*, 336 (859) n→ π*, 460 (1360) CT	470	612 (17.6) CT
3	274(5832) π→π*, 335 (419) n→ π*, 461(710) CT	470	614 (16.5) CT
4	272(7605) π→π*, 336 (673) n→ π*, 459 (747) CT	470	612 (21.3) CT
5	273(6119) π→π*, 336 (446) n→ π*, 460 (757) CT	470	609 (20.4) CT
6	272(8035) π→π*, 334 (766) n→ π*, 459 (963) CT	470	612 (20.8) CT
7	274(5518) π→π*, 333 (519) n→ π*, 460 (661) CT	470	612 (16.6) CT
8	272(8035) π→π*, 336 (785) n→ π*, 459 (1000) CT	470	601 (16.8) CT
9	274(12072) π→π*, 337 (454) n→ π*, 459 (1090) CT	470	606 (23.3) CT

Literature reveals that fluorescence properties of the compounds depends on the molecular arrangements achieved by means of polymorphism, conformational rigidity of the fluorophore (dihedral angles), non-conventional intermolecular interactions as well as on the nature of substituents affecting the photo induced electron transfer processes are well documented in the literature.[32]

7.3.4 Theoretical Investigations.

7.3.4.1 Density functional theory calculations

The geometry of all the compounds **1-9** has been optimized by a DFT level calculations using B3LYP/LanL2DZ basis sets. The optimized structures for the minimum energy conformation of these complexes are presented in Figure 8. Gaussian 6.0 program suite [33] has been used for calculations and molecular orbitals were generated by GaussView 3.0 program. The structural parameters such as bond lengths and bond angles obtained theoretically are found to be consistent with the similar data obtained experimentally (Table 4) which validate the method of optimization.

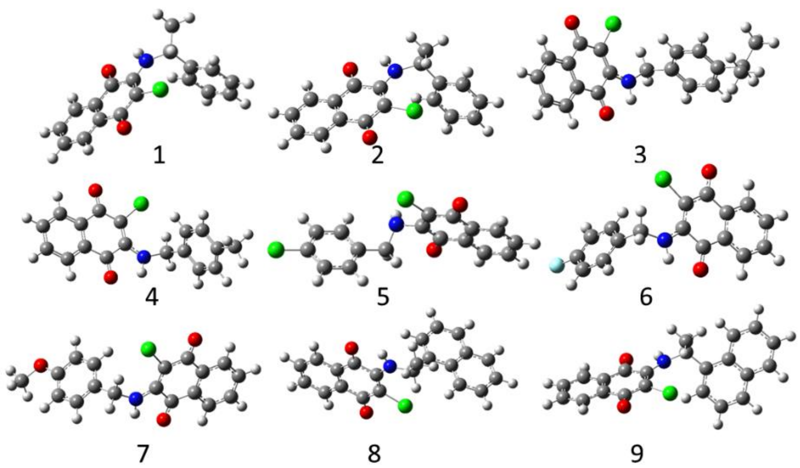

Figure 8. An optimized geometry for the minimum energy conformation of all compounds **1-9** at B3LYP/LanL2DZ level.

The calculated HOMO-LUMO energy gaps (Isovalue = 0.02) for all the compounds **1-9** are given in Table 6 and their localization is illustrated in Figure 9.

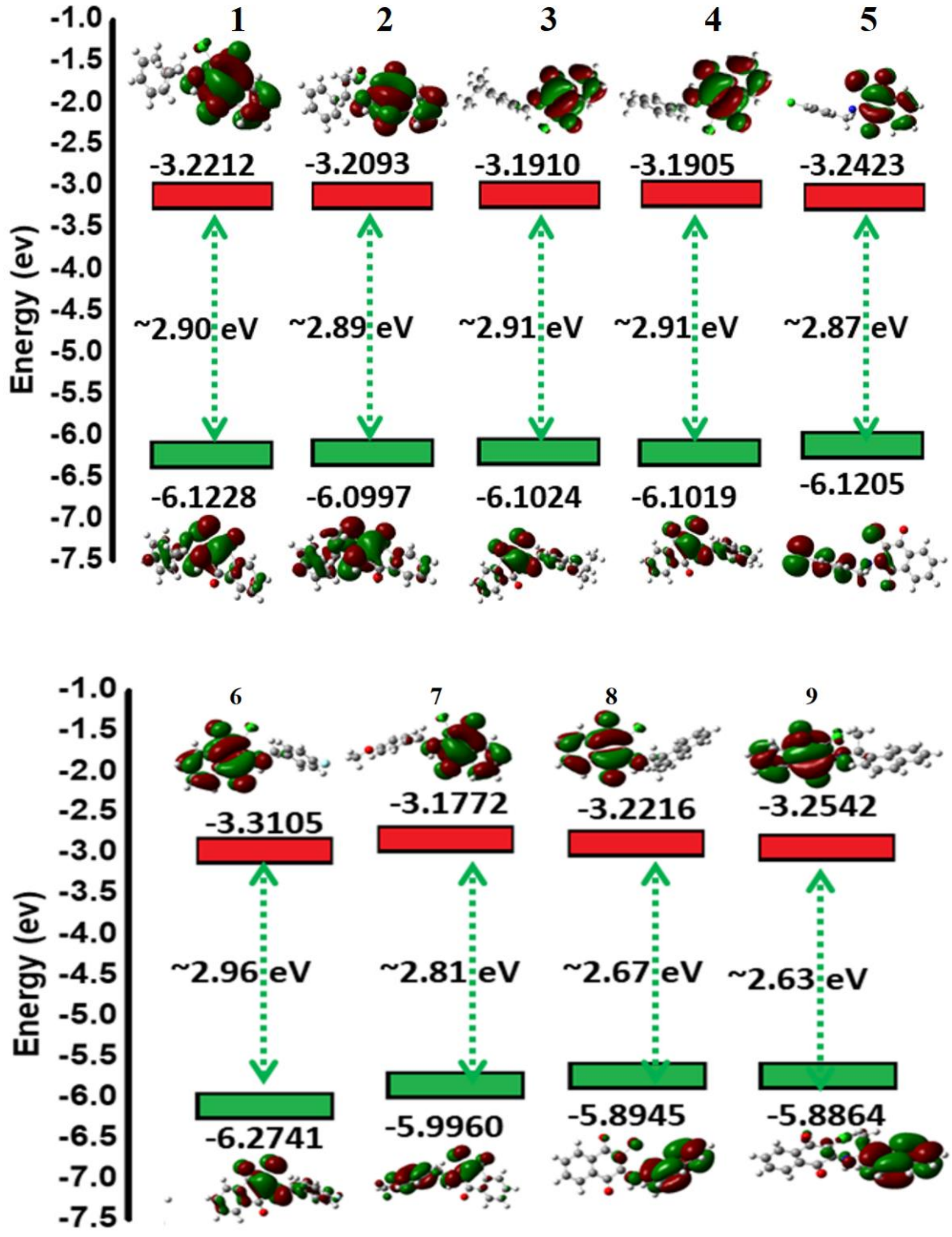

Figure 9. Comparison of the frontier molecular orbitals derived from DFT calculation at the B3LYP/LAN2DZ level for all compounds **1**-**9**.

It may be noted that for compound (1-9), the HOMO is localized over alkyl chain & benzene ring, LUMO is delocalized over naphthalene ring.

Table 6. Summary of Computational study performed on all compounds 1-9.

Code	Energy (Hatree)	HOMO(ev)	LUMO(ev)	Band Gap (eV)
1	-1359.49	-6.1228	-3.2212	2.901
2	-1359.48	-6.0997	-3.2093	2.890
3	-1438.10	-6.1024	-3.1910	2.911
4	-1359.49	-6.1018	-3.1905	2.911
5	-1779.76	-6.1205	-3.2423	2.878
6	-1419.40	-6.2741	-3.3105	2.963
7	-1434.67	-5.9960	-3.1772	2.818
8	-1513.10	-5.8945	-3.2215	2.672
9	-1513.08	-5.8863	-3.2542	2.632

7.3.4.2 Molecular electrostatic potential

Table 6 clearly revealed that all the compounds gave a HOMO-LUMO band gap in 2.63-2.91 eV region, suggestive of their semiconducting nature. Moreover, the molecular electrostatic potential (MESP) of all the compounds (Figure 10) have been determined to provides valuable information about electronic environment of the molecule which would be useful for the prediction of their properties and potential sites for reactivity, including biological systems.[34] Figure 10 suggests the localization of negative potentials majorly around one of the oxygen of naphthoquinone and positive potentials around the variable sites of aromatic/ amino groups. This generates a scope for fine tuning of reactivity of these molecules in the biological system towards amino acids/ proteins.

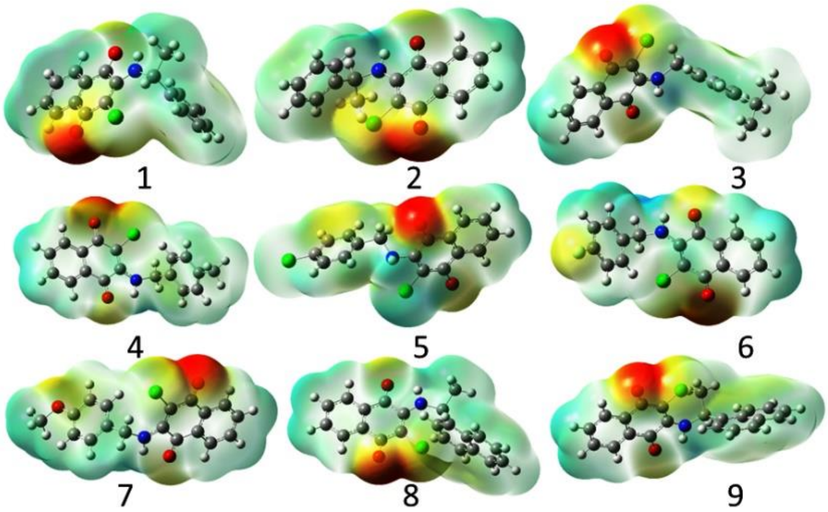

Figure 10. Representations of electron density from total SCF density (Isovalue= 0.0004; mapped with ESP).

Further in-silico study was performed to expose the influence of various N-alkyl substituents and chirality of the pro-drugs **1-9** on the interactions with 1ZXM protein.

7.3.5 Protein- ligand molecular interactions

Naphthoquinone group has been identified as an important pharmacophoric moiety which can exert an antiproliferative effect in cancer cells.[35] Natural or synthetic compounds containing quinone group represent the second largest class of clinically approved anticancer agents.[36] Further reports suggests that a subtle changes in the oxygen-oxygen donor atom system of quinonoidal compounds can have pronounced effects on their coordination tendencies and biological activities.[37] A number of pathways such as intercalation, DNA strand breakage, free radical mediated alkylation and inhibition of DNA repair enzymes are used to explained the cytotoxicities of quinonoidal compounds..[38]

These outcomes encouraged us to understand the binding preference of synthesized compounds with the active site of target protein, ATPase domain of Topoisomerase-II (PDB:1ZXM). ATPase domain of Topoisomerase-II is a major enzyme known to maintain DNA topology, repair, and chromosome condensation/decondensation.[39] The electrophilic and redox-cycling properties of quinone derivatives induces genotoxic, cytotoxic and immunotoxin potentials regulated through the formation of reactive oxygen species and molecular targets including tubulin, topoisomerase II, histone, and DNA. [40]

Evidently, the experimental results of wet lab are found to be in good agreement with the predicted ones as observed from the dock score.[41] This provides useful insights about the structural requirements necessary for carrying out rationally based pharmacophoric modifications in order to obtain promising compounds with anticancer effects.

Molecular docking for protein-ligand studies has been performed to determine the binding mode of synthesized compounds **1-9** with the most probable sites of 1ZXM receptor. Dock scores for each ligand with different poses have been represented in Table 7. Binding interaction of all the newly synthesized compounds with the 1ZXM protein is shown in Figures 11. In general, all the compounds effectively bind to the Asn A: 150, SER A: 149 active sites of ATPase domain of human Topoisomerase-II (1ZXM) with very good dock score of 8.5-10.0 Kcal/mol. Highest dock score is obtained for compound **8** holding chirality at N-alkyl substiuent which binds with 1ZXM protein at the SER A: 149 site and demonstrate its superior efficacy for ligand-protein bonding than the other ligands and proves to be most potent inhibitor.

Table 7. Interaction of ligands with receptor sites of 1ZXM protein.

Ligand	PDB Code	Non-bonding Interactions within 6Å		Binding Energy (Kcal/mol)
		Hydrogen Bonding	Hydrophobic Interaction	
1	1ZXM	Asn A: 150	Ala A:167, Mg A:903, , Arg A:98, Ile A :125	-8.9
2	1ZXM	Asn A: 150	Ala A:167, Mg A:903, Asp A:94, Ile A :125	-8.5
3	1ZXM	-	Ile A:217, Asn A: 95, Ser A: 149, Asn A: 150	-9.1
4	1ZXM	Asn A: 150	Ala A:92, Ala A:167, Mg A:903, Ile A :88, Ile A: 217, Ile A: 118	-9.2
5	1ZXM	Asn A: 150	Ala A:167, Ala A:92, Mg A:903, Ile A:88, Ile A:118, Ile A:217	-9.0
6	1ZXM	Asn A:150	Ala A:167, Ala A:92, Mg A: 903, Ile A:88, Asn A: 120	-8.9
7	1ZXM	Gly A: 166	Ile A:125, Ala A:167, Ala A:92, Asn A: 91	-8.8
8	1ZXM	SER A: 149	Ile A:125, Ile A:141, Lys A: 168, Ala A:167, Mg A:903, Phe A: 142	-10.0
9	1ZXM	-	Asn A: 95, Asn A: 91, Ala A:92, Ile A:125, Ile A:217, Ile A:141	-9.4

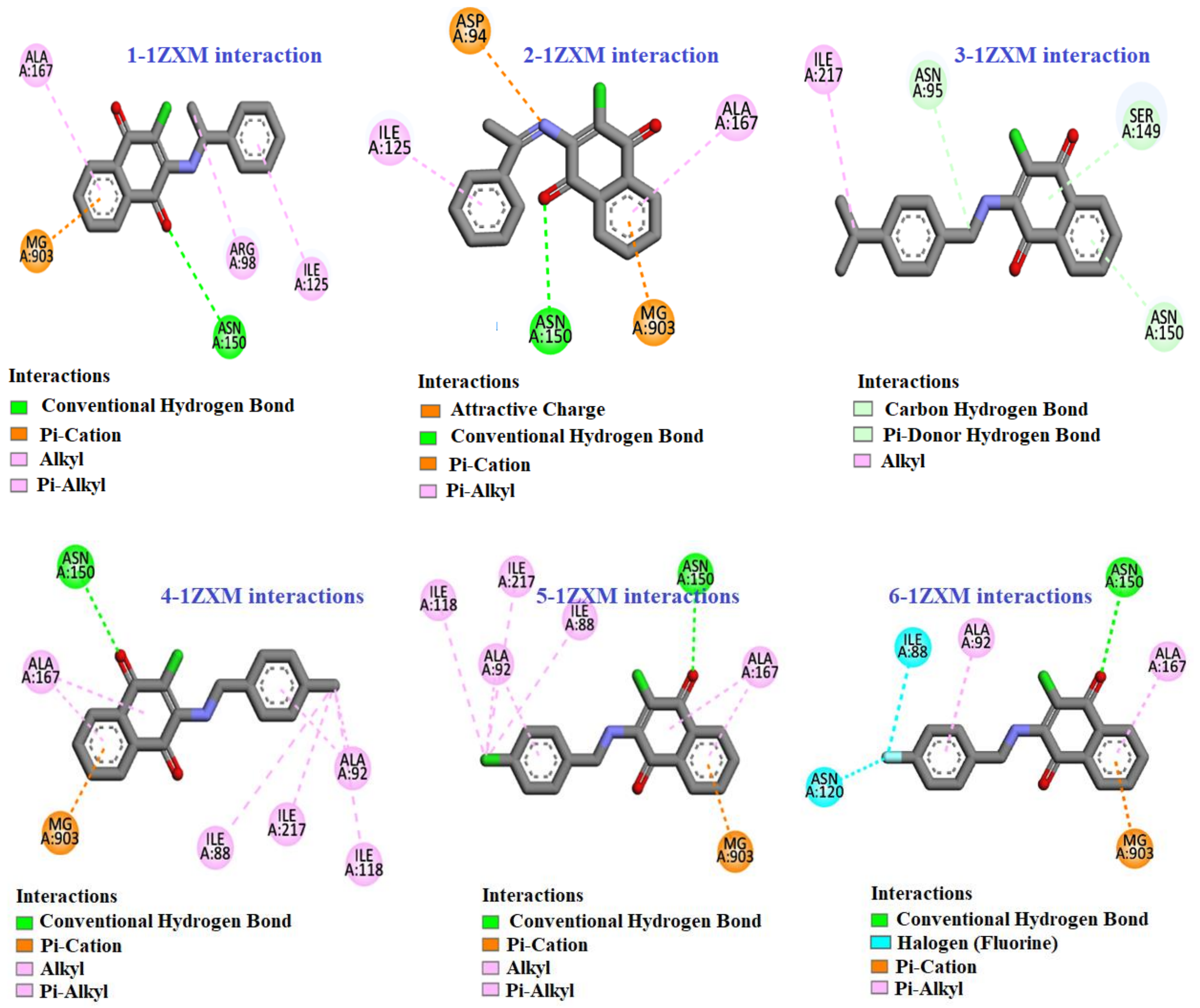

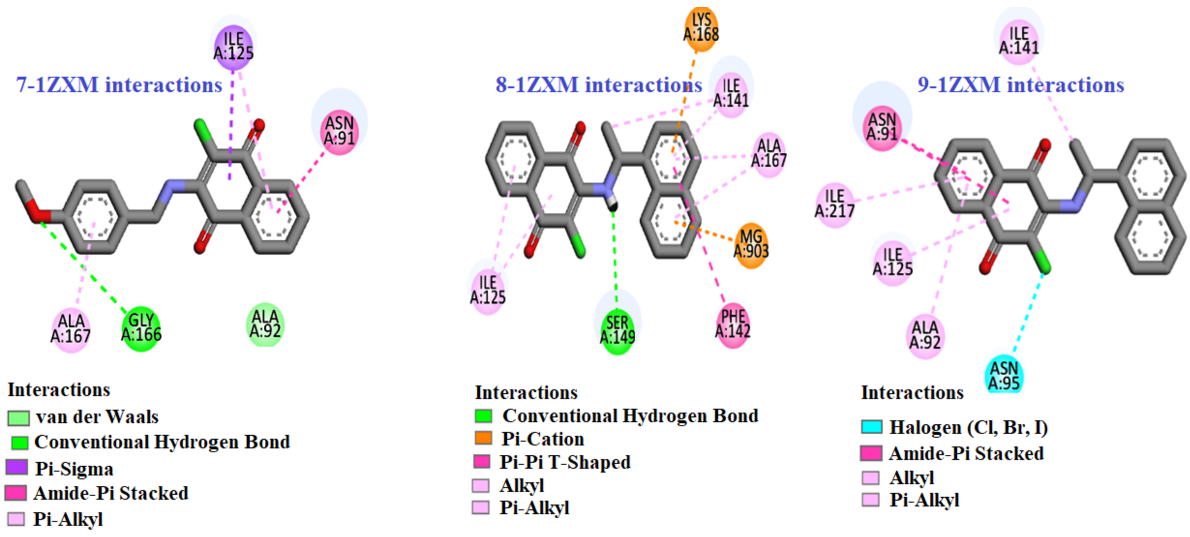

Figure 11. Binding of compounds **1-9** with 1ZXM receptor.

A mechanistic view of inhibition of the ATPase domain of human Topoisomerase-II by 1,4-Benzoquinone, 1,2-Naphthoquinone, 1,4-Naphthoquinone, and 9,10-Phenanthroquinone has been reported by Deepak Gurbani and his co-workers.[42] In silico modelling revealed that Salvicine, a structurally modified diterpenoid quinone, binds with Asn-150, Arg-152, Asn-163, and Gly-164 residues[39] whereas other compounds such as 1,4-benzoquinone, 1,2-naphthoquinone, 1,4- naphthoquinone, and 9,10- phenanthroquinone interacts with Ser-148, Ser-149, Asn-150, and Asn-91 residues[42] of the ATPase domain of human topoisomerase II which is consistent with our results.

7.4 Conclusions

In conclusion, a novel series of chiral/ achiral secondary amine ligands **1-9** holding chirality at *N*-alkyl substituent and naphthoquinone moiety was synthesized and characterized satisfactorily by microanalysis and standard spectroscopy. All the compounds fluoresce in the visible region with concomitant Stokes shifts of ≈ 280 nm. The calculated HOMO-LUMO band gap falls in the range of 2.63-2.91 eV region, suggestive of their semiconducting nature. The unprecedented molecular structure of **1**, **4**, **8** and **9** was determined by means of single-crystal X-ray diffraction (SCXRD) study. The geometry of the compounds has been optimized for their minimum energy conformer by a DFT level calculations. X-ray crystallography along with mapping of molecular electrostatic potential (MESP) reveals the ability of these molecules to offer weak intermolecular interactions. To understand the binding preference of synthesized compounds with the active site of target protein, ATPase domain of Topoisomerase-II (PDB:1ZXM), molecular docking study have been performed. ATPase domain of Topoisomerase-II is reportedly a major enzyme known to maintain DNA topology, repair, and chromosome condensation/decondensation.[39] In general, all the compounds effectively bind to the Asn A: 150, SER A: 149 active sites of ATPase domain of human Topoisomerase-II (PDB ID: 1ZXM) with very good dock score of 8.5-10.0 Kcal/mol. Highest dock score is obtained for compound **8** holding chirality at N-alkyl substituent which binds with 1ZXM protein at the SER A: 149 site and demonstrate its superior efficacy for ligand-protein bonding than the other ligands and proves to be most potent enzyme inhibitor. The overall interaction of these ligands with sites of 1ZXM protein is found to be consistent with reported interaction of Salvicine, a structurally modified diterpenoid quinone with Asn-150, Arg-152, Asn-163, and Gly-164 residues. [39] These compounds are more likely to move on to higher phases of the drug development process to obtain promising compounds with anticancer effects.[35]

7.5 Reference

[1] (a) S. L. de Castro, F. S. Emery, E. N. da Silva Júnior, *Eur. J. Med. Chem.*, **2013**, 69, 678; (b) V. F. Ferreira, S. B. Ferreira, F. d. C. da Silva, *Org. Biomol. Chem.*, **2010**, 8, 4793; (c) D. A. Lanfranchi, E. C. -Rodo, B. Bertrand, H. –H. Huang, L. Day, L. Johann, M. Elhabiri, K. Becker, D. L. Williams, E. D. -Charvet, *Org. Biomol. Chem.*, **2012**, 10, 6375; (d) V. R. Campos, E. A. dos Santos, V. F. Ferreira, R. C. Montenegro, M. C. B. V. de Souza, L. V. C. -Lotufo, M. O. de Moraes, A. K. P. Regufe, A. K. Jordao, A. C. Pinto, J. A. L. C. Resende, A. C. Cunha, *RSC Advances*, **2012**, 2, 11438; (e) V. K. Tandon, H. K. Maurya, M. K. Verma, R. Kumar, P. K. Shukla, *Eur. J. Med. Chem.*, **2010**, 45, 2418.

[2] N. El-Najjar, H. Gali-Muhtasib, R. A. Ketola, P. Vuorela, A. Urtti, H. Vuorela, *Phytochem. Rev.*, **2011**, 10, 353.

[3] (a) D. W. Lamson, S. M. Plaza, *Med. Rev.*, **2003**, 8, 303; (b) Y. Ohsaki, H. Shirakawa, K. Hiwatashi, Y. Furukawa, T. Mizutani, M. Komai, *Biosci. Biotechnol. Biochem.*, **2006**, 70, 926.

[4] (a) T. Kayashima, M. Mori, H. Yoshida, Y. Mizushina, K. Matsubara, *Cancer Lett.*, **2009**, 278, 34; (b) 20 D. Aminin, S. Polonik, *Chem. Pharm. Bull.*, **2020**, 68, 46.

[5] (a) M. J. Hossen, W. S. Yang, D. Kim, A. Aravinthan, J. H. Kim, J. Y. Cho, *Sci. Rep.*, **2017**, 7, 42995; (b) M. Imran, A. Rauf, I. A. Khan, M. Shahbaz, T. B. Qaisrani, S. Fatmawati, T. Abu-Izneid, A. Imran, K. U. Rahman, T. A. Gondal, *Pharmacother.*, **2018**, 106, 390.

[6] (a) J. W. Han, D. W. Shim, W. Y. Shin, K. H. Heo, S. B. Kwak, E. J. Sim, J. H. Jeong, T. B. Kang, K. H. Lee, *Int. J. Mol. Sci*., **2015**, 16, 8102; (b) W. T. Wei, S. Z. Lin, D. L. Liu, Z. H. Wang, *Oncol. Rep*., **2013**, 30, 2555.

[7] (a) R. S. Peres, G. B. Santos, N. T. Cecilio, V. A. Jabor, M. Niehues, B. G. Torres, G. Buqui, C. H. Silva, T. D. Costa, N. P. Lopes, M. C. Nonato, F. S. Ramalho, P. Louzada-Júnior, T. M. Cunha, F. Q. Cunha, F. S. Emery, J. C. Alves-Filho, *Arthritis Res Ther*., **2017**, 47; (b) F. Epifano, S. Genovese, S. Fiorito, V. Mathieu, R. Kiss, *Phytochem. Rev*., **2014**, 13, 37.

[8] (a) P. Luo, Y. F. Wong, L. Ge, Z. F. Zhang, Y. Liu, L. Liu, H. Zhou, *J. Pharmacol. Exp. Ther*., **2010**, 335, 735; (b) Y. Y. Cao, J. Yu, T. T. Liu, K. X. Yang, L. Y. Yang, Q. Chen, F. Shi, J. J. Hao, Y. Cai, M. R. Wang, W. H. Lu, Y. Zhang, *Cell Death Dis*., **2018**, 9, 17.

[9] A. Seetha, H. Devaraj, G. Sudhandiran, *J. Biochem. Mol. Toxicol*., **2020**, 34, e22433.

[10] P. L. Liao, C. H. Lin, C. H. Li, C. H. Tsai, J. D. Ho, G. C. Chiou, J. J. Kang, Y. W. Cheng, *Sci Rep*., **2017**, 7, 44985.

[11] (a) G. Powis, *Pharmacol. Ther*., 1987, **35**, 57; (b) P. J. O'Brien, *Chem. Biol. Interact*., 1991, **80**, 1; (c) Ismail Sami Mahmoud, Ma'mon M. Hatmal, Duaa Abuarqoub, Ezaldeen Esawi, Hiba Zalloum, Suha Wehaibi, Hamdi Nsairat, Walhan Alshaer, *ACS Omega*, **2021**, 6, 25299.

[12] (a) V. K. Tandon, R. V. Singh, D. B. Yadav, *Bioorganic & Medicinal Chemistry Letters*, **2004**, 14, 2901; (b) O'Brien, P. *J. Chem. Biol. Interact*., **1991**, 80, 1.

[13] (a) J. R. E. Hoover and A. R. Dag, *J. Am. Chem. Soc.*, **1954**, 76, 4148; (b) S. A. Vichkanova, S. B. Izosimova, V. V. Adgina, L. D. Shipulina, *Rastitel'nye Resursy,* **1979**, 15, 167; (c) N. G. Clark, *Pestic. Sci.*, **1985**, 16, 23; (d) V. K. Tandon, H. K. Maurya, A. Tripathi, G. B. ShivaKesva, P. K. Shukla, A. Srivastava, D. Panda, *Eur. J. Med. Chem*., **2009**, 44, 1086; (e) V. K. Tandon, H. K. Maurya, D. B. Yadav, A. Tripathi, M. Kumar and P. K. Shukla, *Bioorg. Med. Chem. Lett.*, **2006**, 16, 5883. (f) P. Ravichandiran, M. Masłyk, S. Sheet, M. Janeczko, D. Premnath, A. R. Kim, B. Park, M. Han, D. J. Yoo, *ChemistryOpen*, **2019**, 8, 589.

[14] (a) K. W. Stagliano, A. Emadi, US20040087663A1 **2004**; (b) S. Ganapaty, P. S. Thomas, G. Karagianis, P. G. Waterman, R. Brun, *Phytochemistry*, **2006**, **67**, 1950.

[15] C. Biot, H. Bauer, R. H. Schirmer, E. D. -Charret, *J. Med. Chem*., **2004**, 47, 5972.

[16] (a) A. B. Pardee, Y. Z. Li, C. J. Li, *Cancer Drug Targets*, **2002**, 2, 227; (b) B. Hazra, M. D. Sarma, U. Sanyal, *J. Chromatogr. B Anal. Technol. Biomed. Life Sci*., **2004**, 812, 259.

[17] R. Song, B. Yu, Dirk Friedrich, J. Li, H. Shen, H. Krautscheid, S. D. Huang, M. Kim, *Commun Biol*, **2020,** 3, 529.

[18] F. R. F. Dias, J. S. Novais, T. A. d. N. S. Devillart, W. A. da Silva, M. O. Ferreira, R. D. S. Loureiro, V. R. Campos, V. F. Ferreira, M. C. B. V. de Souza, H. C. Castro, A. C. Cunha, *Eur. J. Med. Chem*., **2018**, 156, 1.

[19] V. K. Singh, S. K. Verma, R. Kadu, S. M. Mobin, RSC Advances, **2015**, 5, 43669.

[20] (a) K.Rissanen, *CrystEngComm*, **2008**, 10, 1107; (b) S. Yamada, N. Sako, M. Okuda, A. Hozumi, *CrystEngComm*, **2013**, 15, 199.

[21] Y. Imai, Y. Inoue, I. Nakanishi, K. Kitaura, *Protein Sci*., **2008**, 17,

[22] 1129 L. Brammer, G. M. Espallagras, S. Libri, *CrystEngComm*, **2008**, 10, 1712.

[23] (a) K. Bouchmella, B. Boury, S. G. Dutremez and A. van der Lee, *Chem. Eur. J.*, **2007**, **13**, 6130; (b) C. B. Aakeroy, M. Fasulo, N. Schultheiss, J. Desper, C. Moore, *J. Am. Chem. Soc*., **2007**, 129, 13772.

[24] G. M. Espallargas, F. Zordan, L. A. Marin, H. Adams, K. Shankland, J. van der Streek, L. Brammer, *Chem. Eur. J*., **2009**, 15, 7554.

[25] Oxford Diffraction, CrysAlis PRO, Oxford Diffraction Ltd., Yarnton, England, **2009**.

[26] G. M. Sheldrick, SHELXTL Reference Manual: Version 5.1, Bruker AXS, Madison, WI, **1997**.

[27] G. M. Sheldrick, SHELXL-97: Program for Crystal Structure Refinement, University of Göttingen, Göttingen, Germany, **1997**.

[28] N. M. O'Boyle, M. Banck, C. A. James, C. Morley, T. Vandermeersch, G. R. Hutchison, "Open Babel: An open chemical toolbox. *J. Cheminf*., **2011**, 3, 33.

[29] R. Huey, G. M. Morris, A. J. Olson, D. S. Goodsell, *J. Computational Chem*., **2007,** 28, 1145.

[30] (a) S. Pal, M. Jadhav, T. Weyhermuller, Y. Patil, M. Nethaji, U. Kasabe, L. Kathawate, V. B. Konkimalla, S. S. Gawali, *J. Mol. Struct*., 2013, **1049**, 355; (b) J. C. Knight, T. Tatchell and I. A. Fallis, *Acta Cryst*., **2007**, *E63*, o1226.

[31] R. Destro, E. Sartirana, L. Loconte, R. Soave, P. Colombo, C. Destro, L. L. Presti, *Cryst. Growth Des.*, **2013**, 13, 4571.

[32] (a) S. K. Verma, V. K. Singh, *RSC Adv*., **2015**, 5, 53036. (c) S. K Verma, C. Savani, V. K. Singh, *ChemistrySelect*, *2019*, 4, 14244; (b) W. Thongyod, C. Buranachai, T. Pengpan and C. Punwong, *Phys. Chem. Chem. Phys.*, **2019**, 21, 16258; (d) S. C. Martens, U. Zschieschang, H. Wadepohl, H. Klauk and L. H. Gade, *Chem. Eur. J.*, **2012**, 18, 3498. (e) C. Moretti, X. Tao, L. Koehl and V. Koncar, *Smart Textiles and their*

Applications, **2016**, 539; (f) M. T. Qamar, M. Aslam, I. M. I. Ismail, N. Salah, A. Hameed, *ACS Appl. Mater. Interfaces*, **2015**, 7, 8757; (g) H. Hamad, M. M. Elsenety, W. Sadik, A. -G. El-Demerdash, A. Nashed, A. Mostafa, S. Elyamny, *Sci. Rep.*, **2022**, 12, 2217.

[33] M. J. Frisch, G. W. Trucks, H. B. Schlegel, G. E. Scuseria, M. A. Robb, J. R. Cheeseman, G. Scalmani, V. Barone, G. A. Petersson, H. Nakatsuji, X. Li, M. Caricato, A. V. Marenich, J. Bloino, B. G. Janesko, R. Gomperts, B. Mennucci, H. P. Hratchian, J. V. Ortiz, A. F. Izmaylov, J. L. Sonnenberg, D. Williams-Young, F. Ding, F. Lipparini, F. Egidi, J. Goings, B. Peng, A. Petrone, T. Henderson, D. Ranasinghe, V. G. Zakrzewski, J. Gao, N. Rega, G. Zheng, W. Liang, M. Hada, M. Ehara, K. Toyota, R. Fukuda, J. Hasegawa, M. Ishida, T. Nakajima, Y. Honda, O. Kitao, H. Nakai, T. Vreven, K. Throssell, J. A. Montgomery, Jr., J. E. Peralta, F. Ogliaro, M. J. Bearpark, J. J. Heyd, E. N. Brothers, K. N. Kudin, V. N. Staroverov, T. A. Keith, R. Kobayashi, J. Normand, K. Raghavachari, A. P. Rendell, J. C. Burant, S. S. Iyengar, J. Tomasi, M. Cossi, J. M. Millam, M. Klene, C. Adamo, R. Cammi, J. W. Ochterski, R. L. Martin, K. Morokuma, O. Farkas, J. B. Foresman, and D. J. Fox, Gaussian, Inc., Wallingford CT, **2016**.

[34] (a) F. A. Bulat, A. T.-Labbe, T. Brinck, J. S. Murray and P. Politzer, *J Mol Model*, **2010**, 16, 1679; (b) P. Politzer, P. R. Laurence, K. Jayasuriya, *Environ. Health Perspect.*, **1985**, 61, 191.

[35] (a) Bipul R. Acharya, Bhabatarak Bhattacharyya and Gopal Chakrabarti, *Biochemistry*, **2008**, 47, 7838; (b) A. A. Nechaev, P. R. Jagtap, E. Bažíková, J. Neumannová, I. Císařová, E. Matoušová, *Org. Biomol. Chem.*, **2021**, 19, 3434; (c) K. K. Liu, J. Li, S. Sakya, *Mini Rev Med Chem*, **2004**, 4, 1105.

[36] G. Powis, M. P. Hacker, The toxicity of anticancer drugs. New York: Pergamon Press, **1991**, 106.

[37] Z. Afrasiabi, E. Sinn, J. Chen, Y. Ma, A. L. Rheingold, L. N. Zakharov, N. Rath, S. Padhy, *Inorg Chim Acta*, **2004**, 357, 271.

[38] A. Halinska, T. Belej, P. O'Brien. *Br J Cancer Suppl*, **1996**, 27, S23.

[39] D. A. Eastmond, S. T. Mondrala, L. Hasegawa, *Chem. Biol. Interact*. **2005,** 153.

[40] M. Shinyashiki, A. Eiguren-Fernandez, D. A. Schmitz, E. Di Stefano, N. Li, W. P. Linak, S. H. Cho, J. R. Froines, A. K. Cho, *Environ. Res.* **2009**, 109, 239.

[41] S. Shukla, R. S. Srivastava, S. K. Shrivastava, A. Sodhi, P. Kumar, *Journal of Enzyme Inhibition and Medicinal Chemistry*, **2013**, 28,1192.

[42] D. Gurbani, V. Kukshal, J. Laubenthal, A. Kumar, A. Pandey, S. Tripathi, A. Arora, S. K. Jain, R. Ramachandran, D. Anderson, A. Dhawan, *Toxicological Sciences*, **2012**,126, 372.

7.6 Annexures

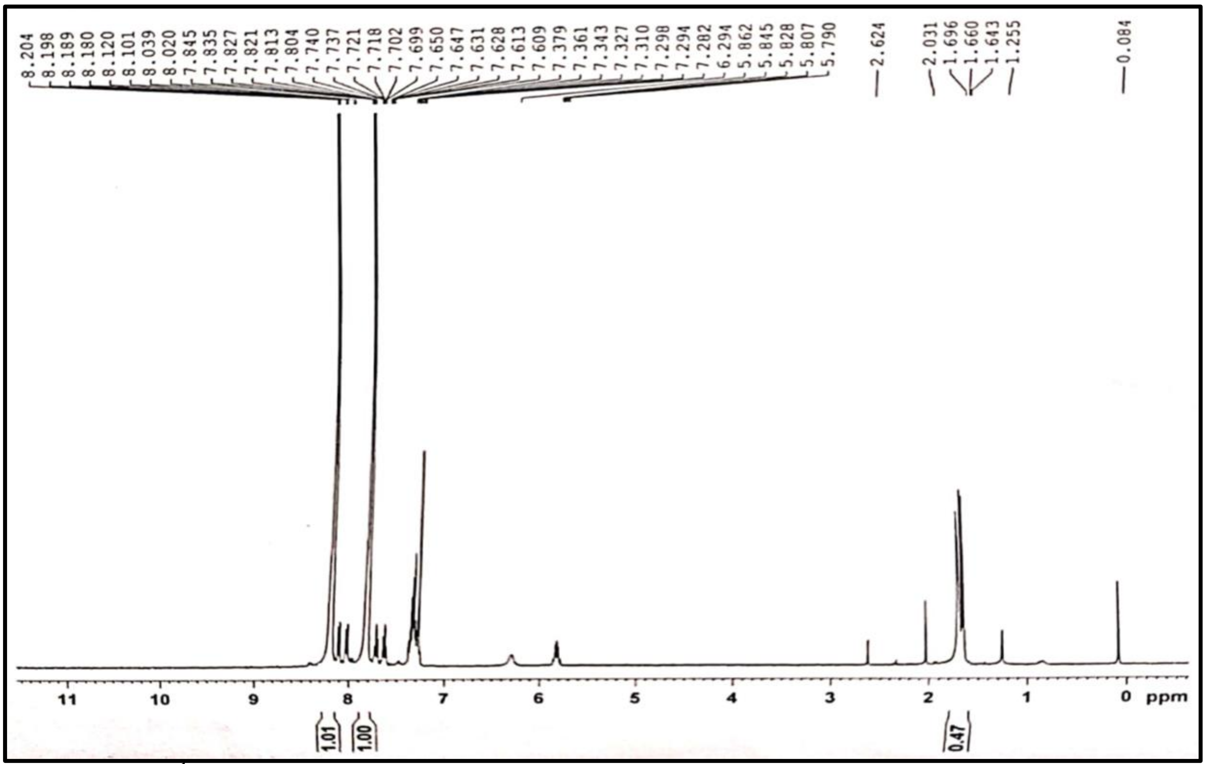

Annexure 1. [1]H NMR spectrum of 1.

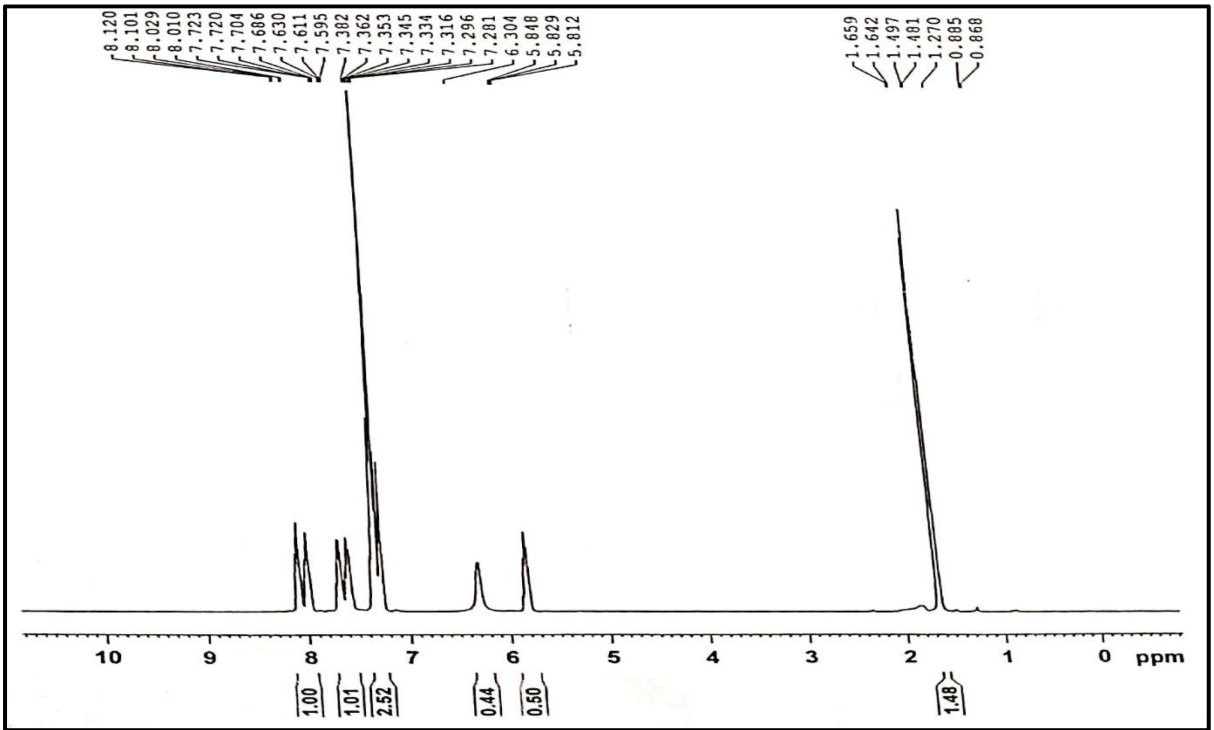

Annexure 2. [1]H NMR spectrum of 2.

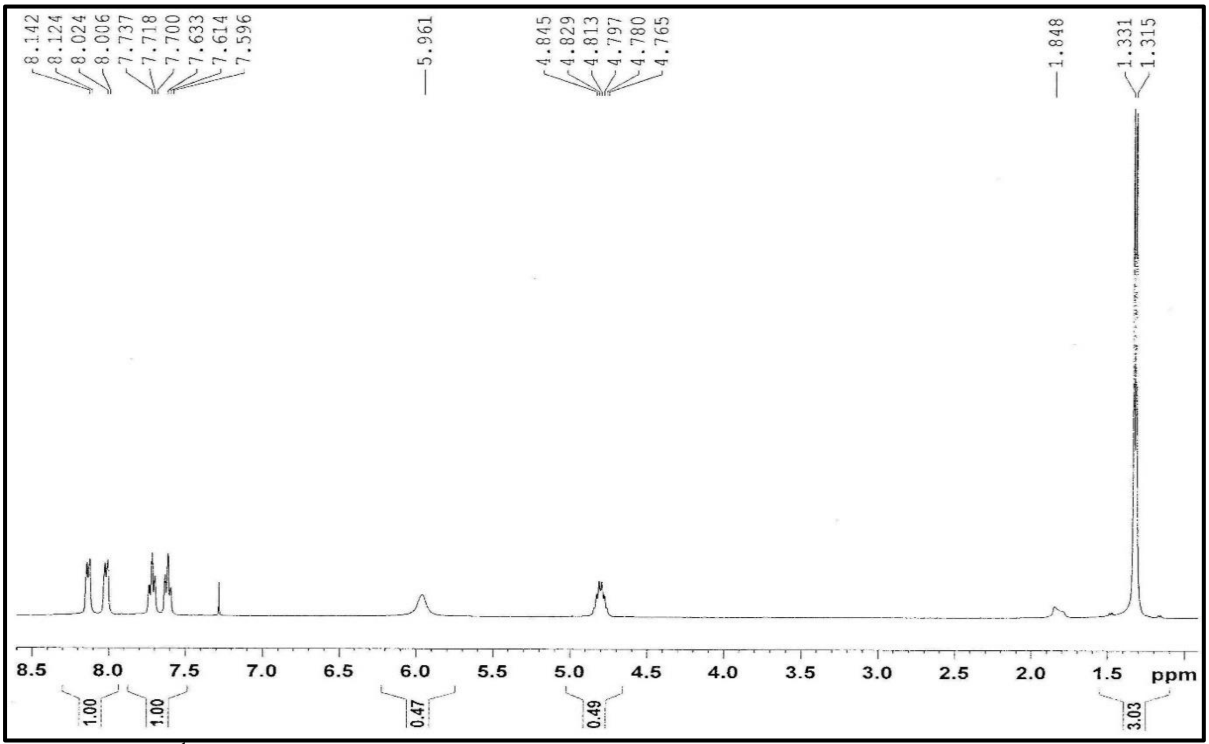

Annexure 3. ^{1}H NMR spectrum of 3.

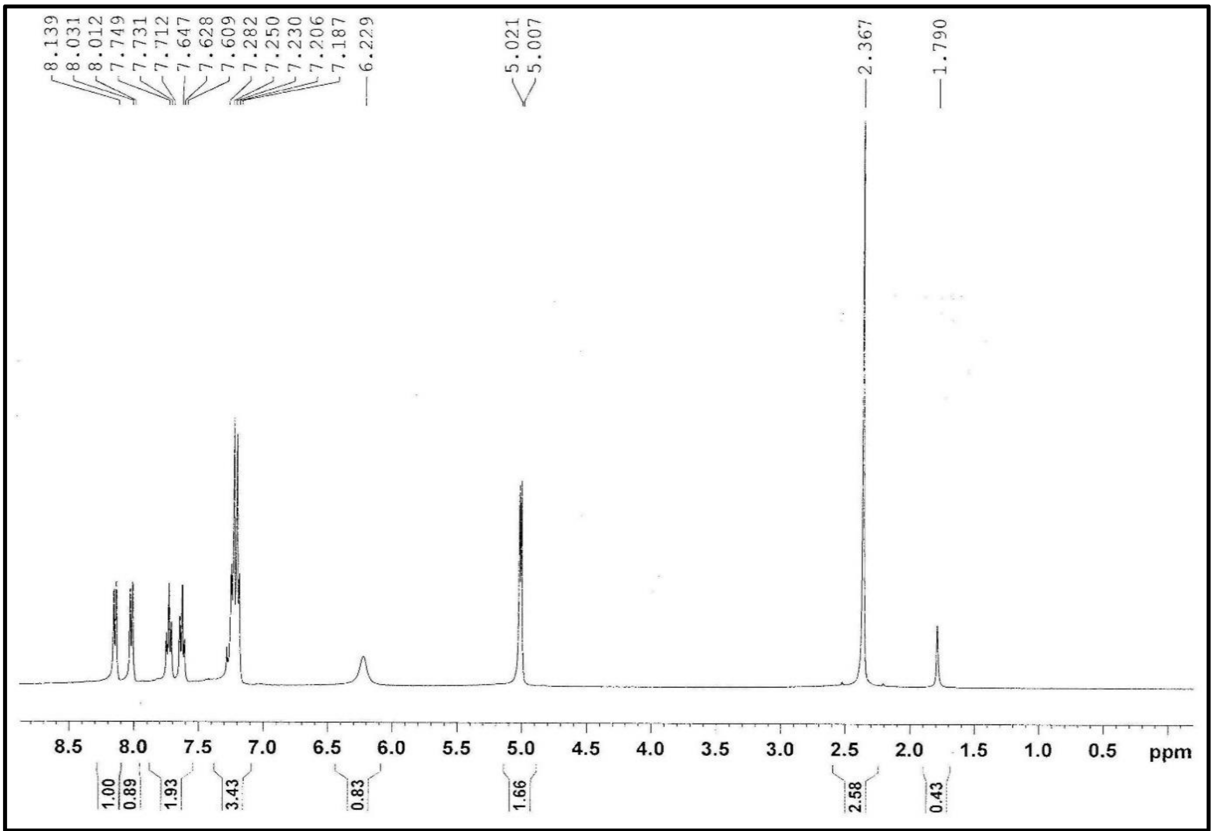

Annexure 4. ^{1}H NMR spectrum of 4.

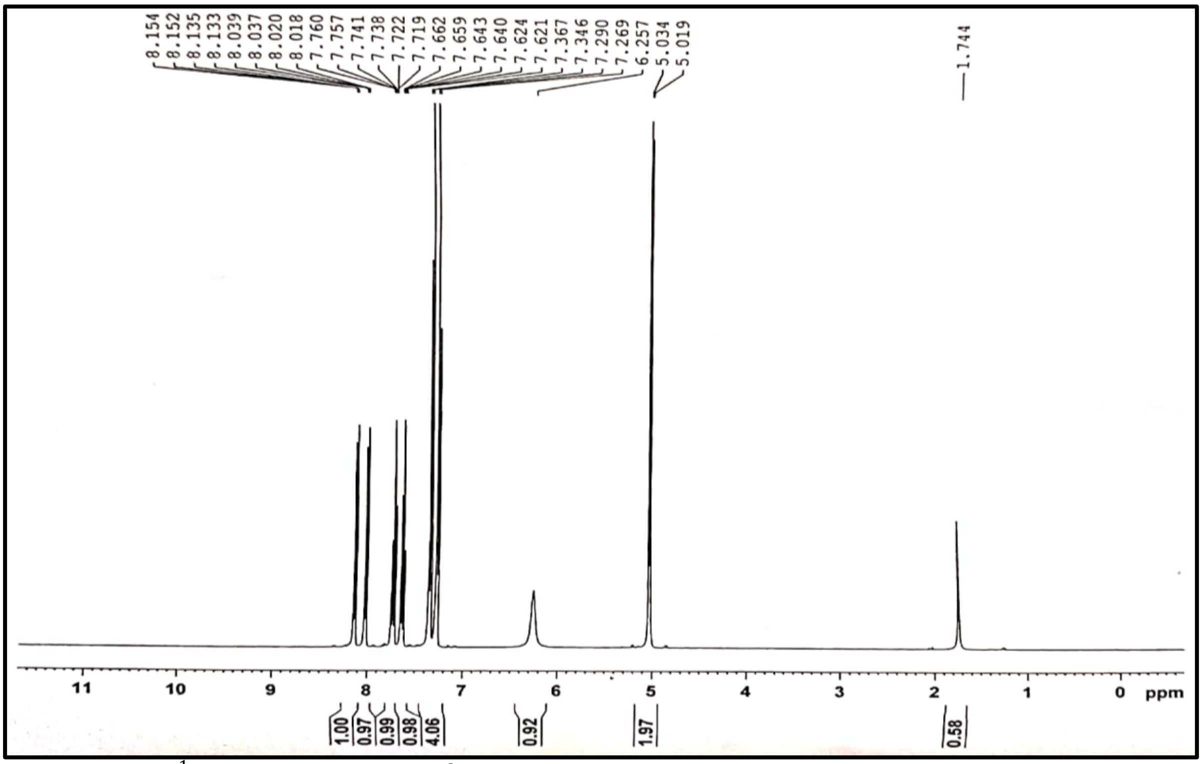

Annexure 5. ^{1}H NMR spectrum of 5.

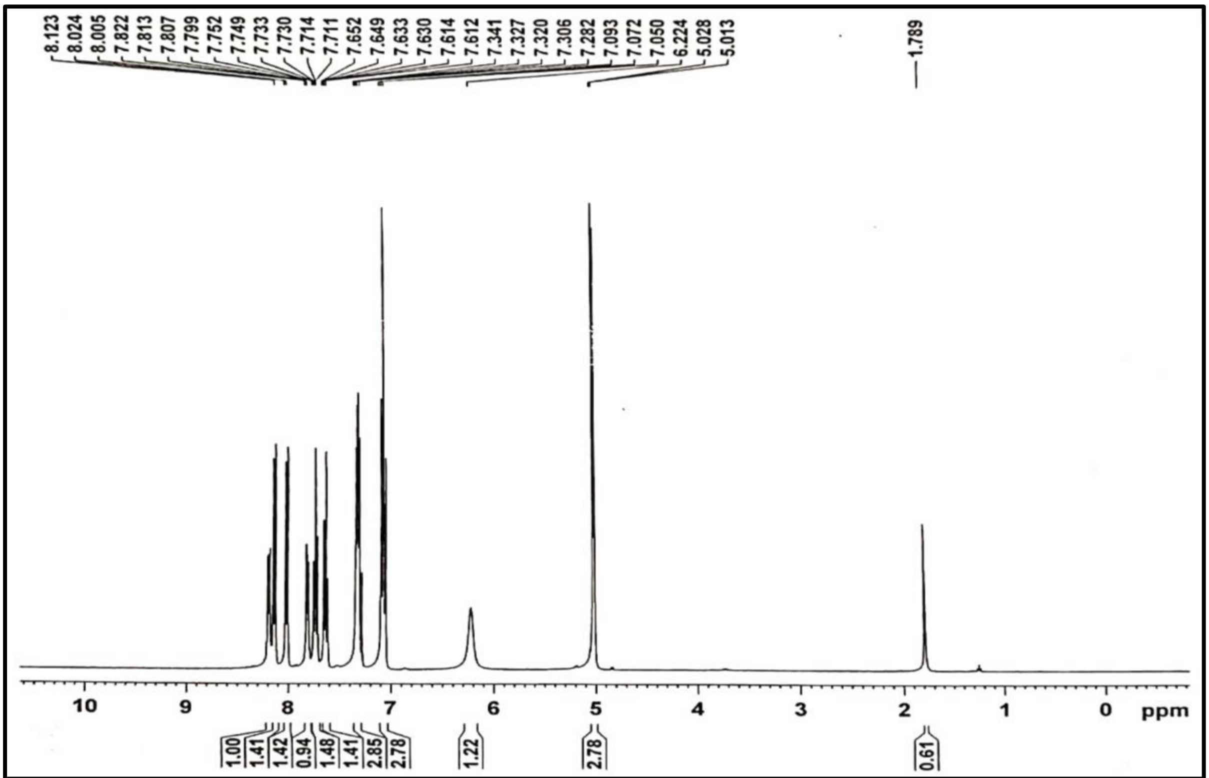

Annexure 6. ^{1}H NMR spectrum of 6.

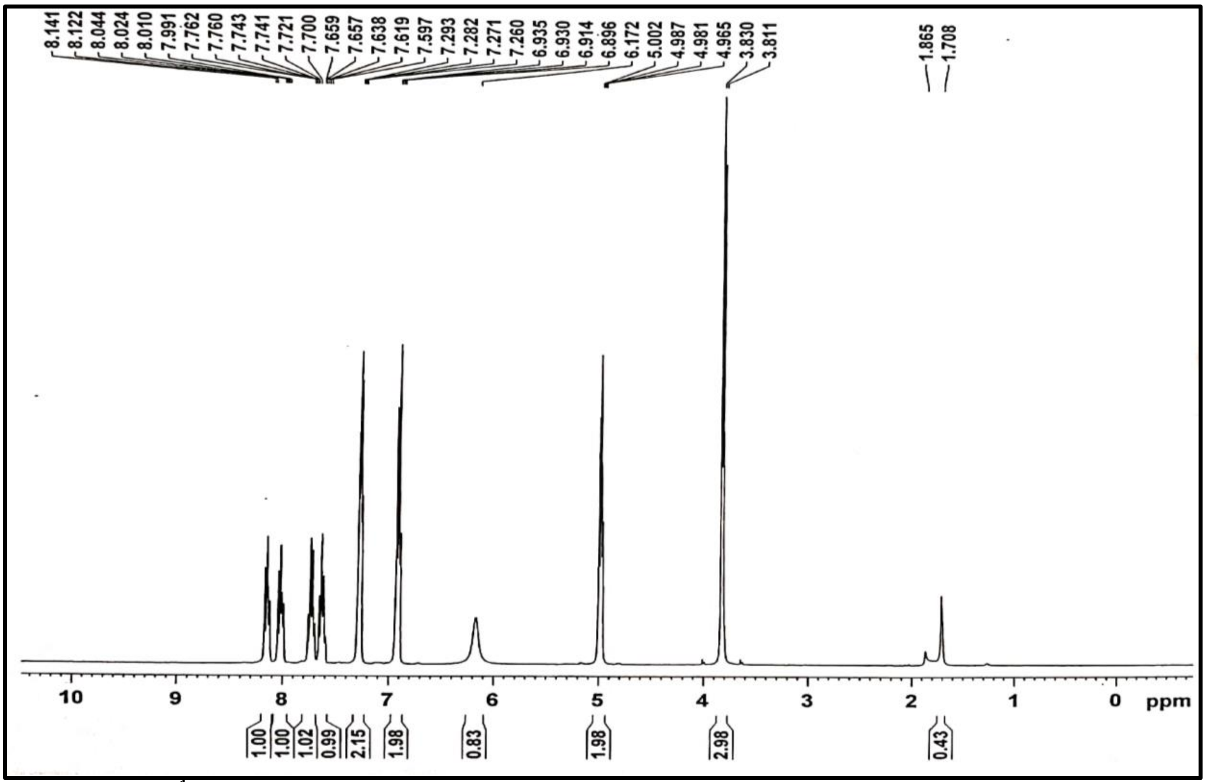

Annexure 7. [1]H NMR spectrum of 7.

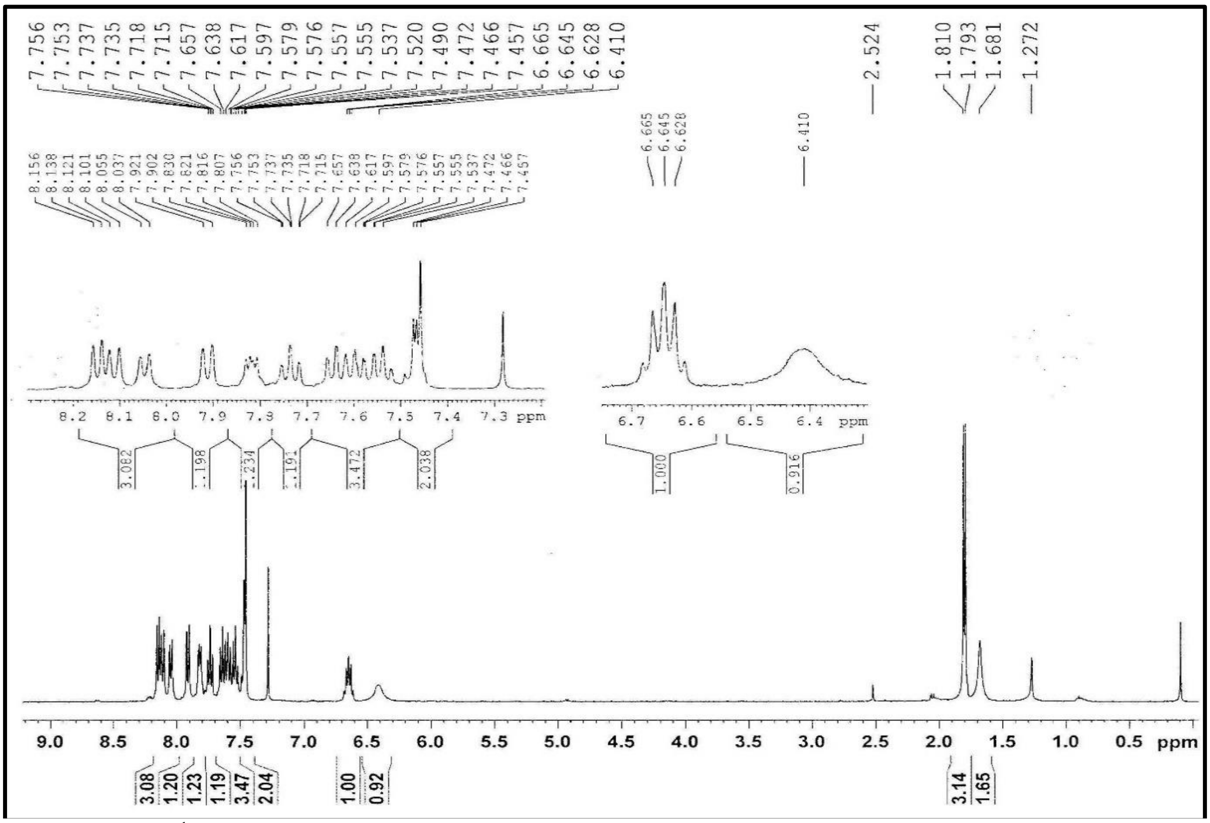

Annexure 8. [1]H NMR spectrum of 8.

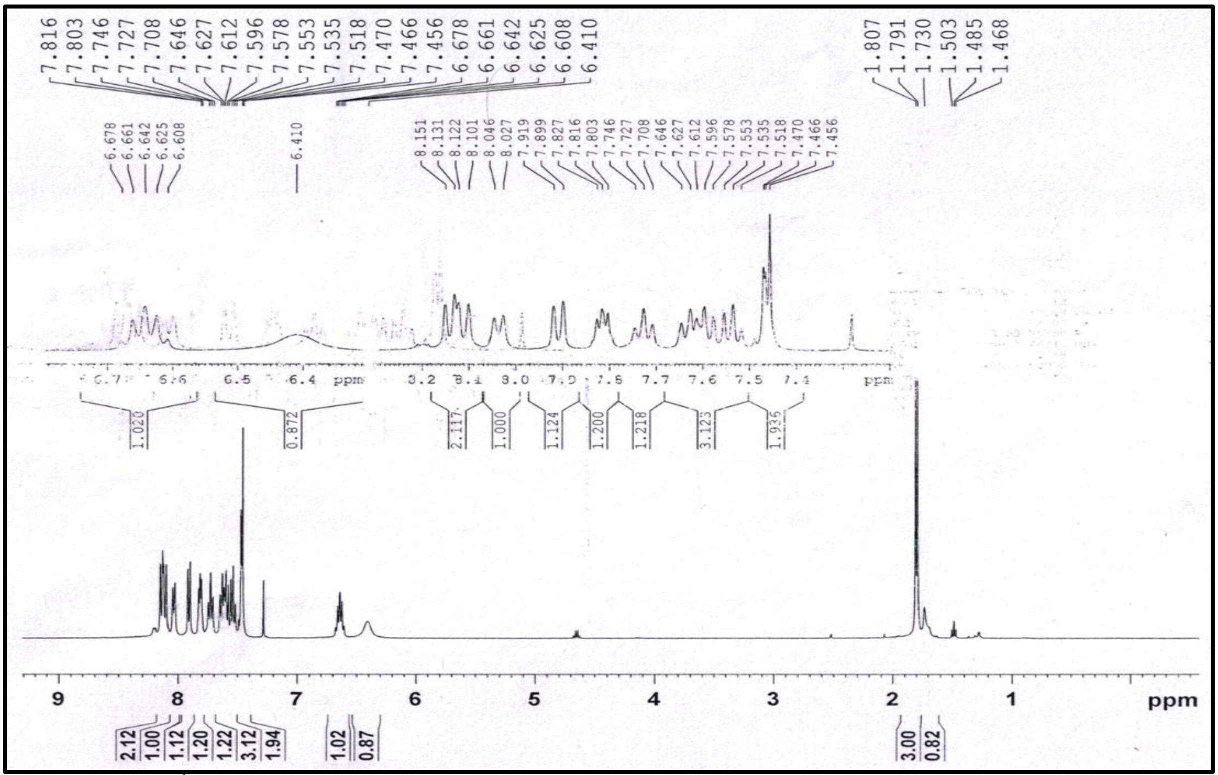

Annexure 9. ^{1}H NMR spectrum of 9.

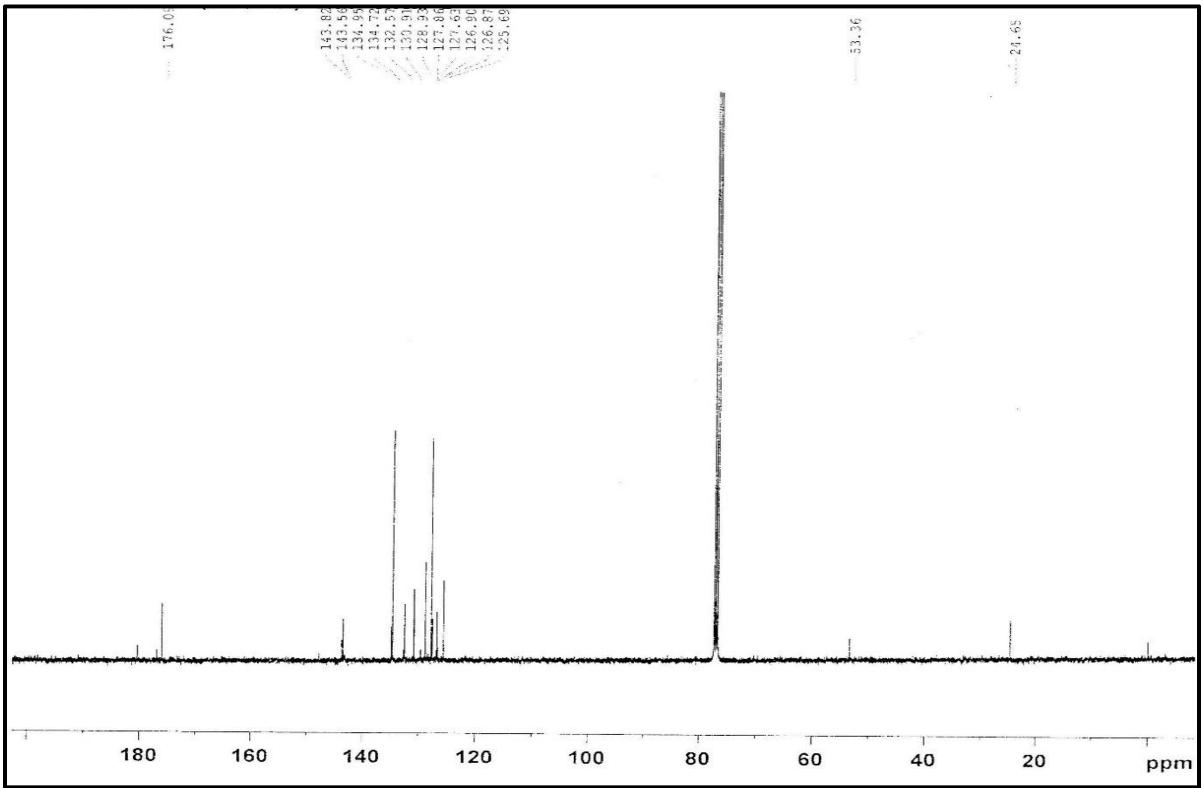

Annexure 10. ^{13}C NMR spectrum of 1.

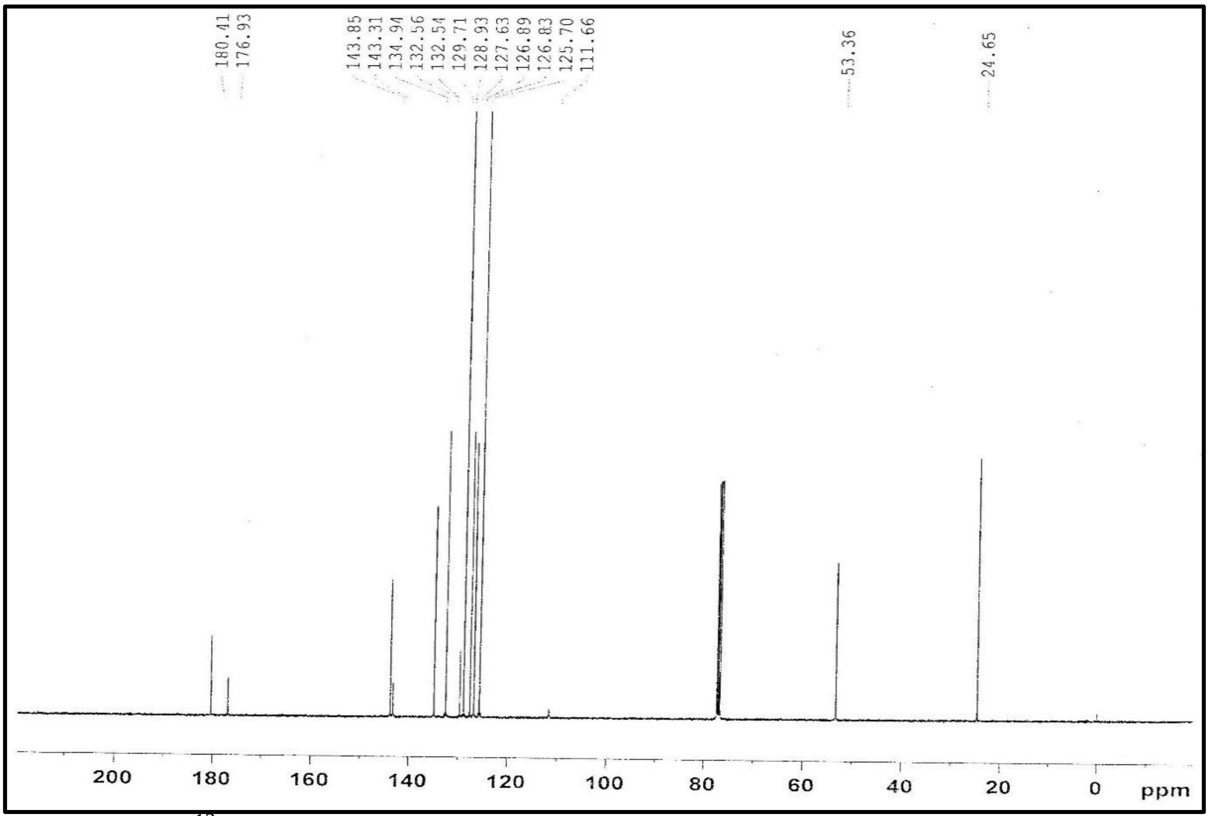

Annexure 11. ^{13}C NMR spectrum of 2.

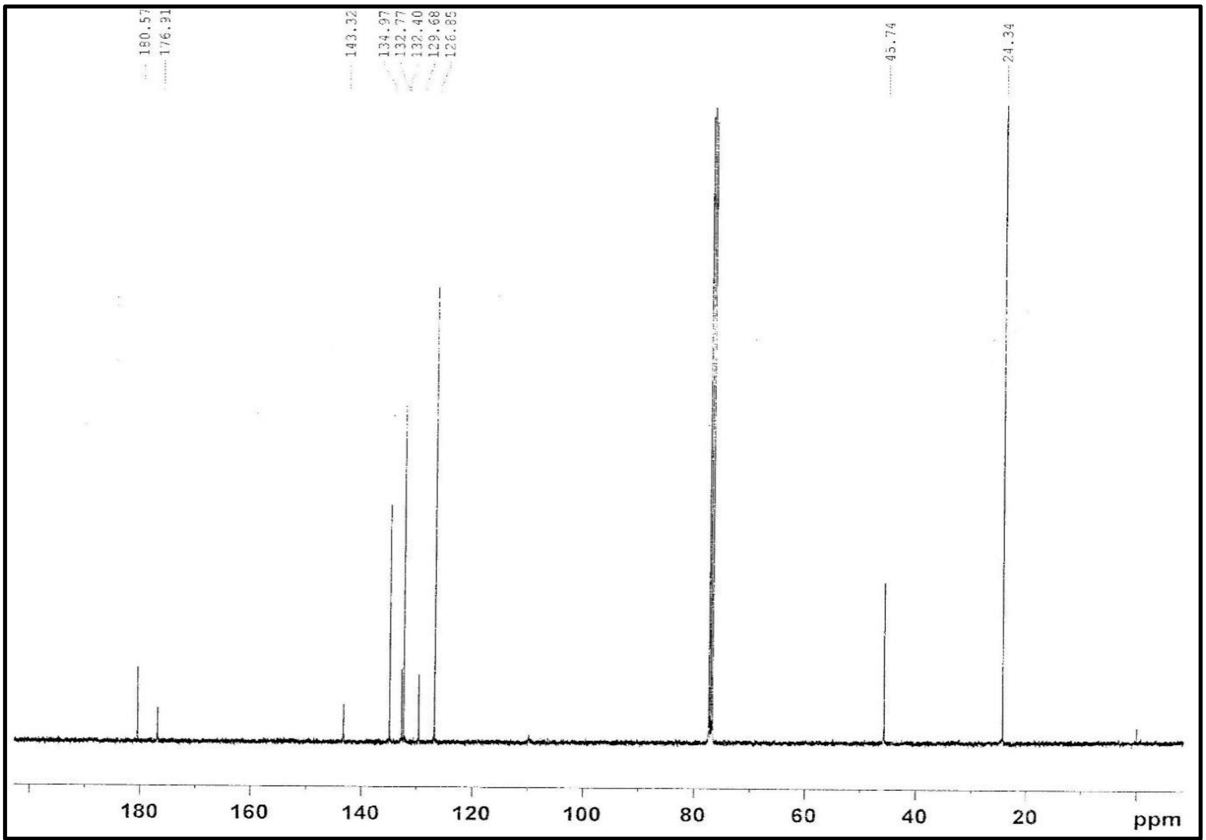

Annexure 12. ^{13}C NMR spectrum of 3.

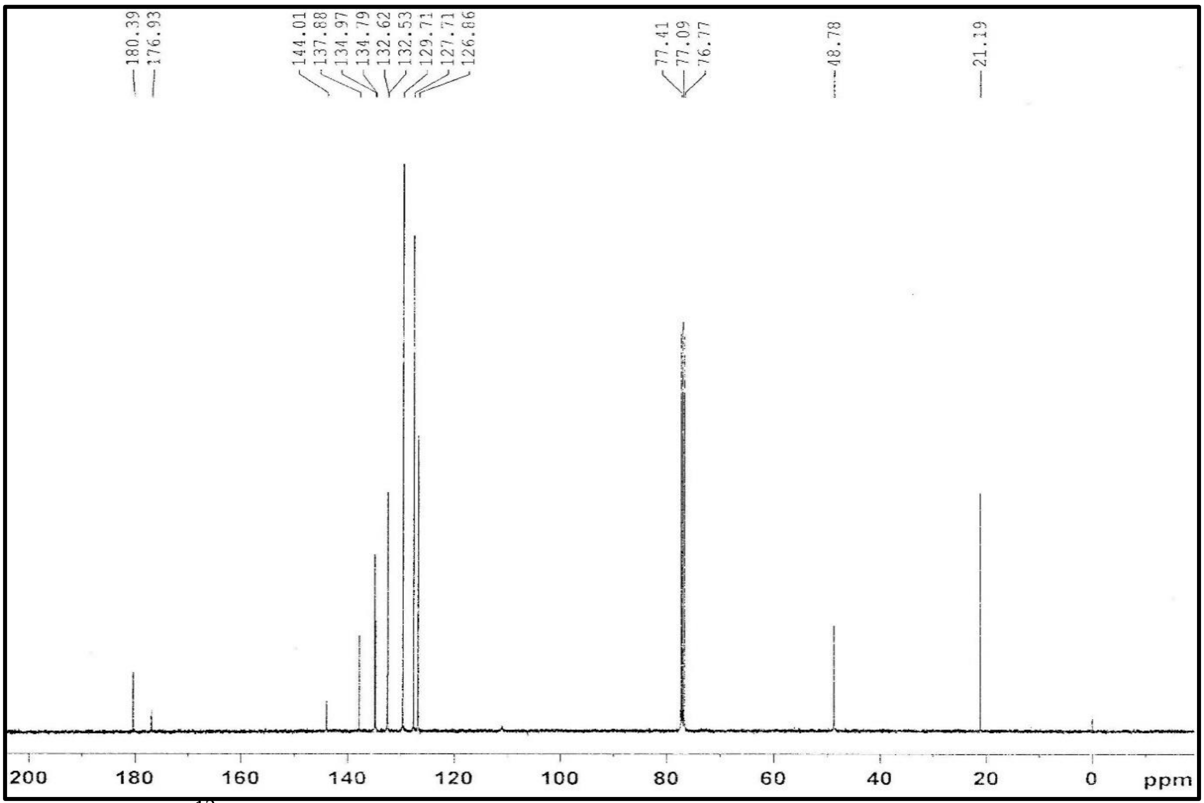

Annexure 13. ^{13}C NMR spectrum of 4.

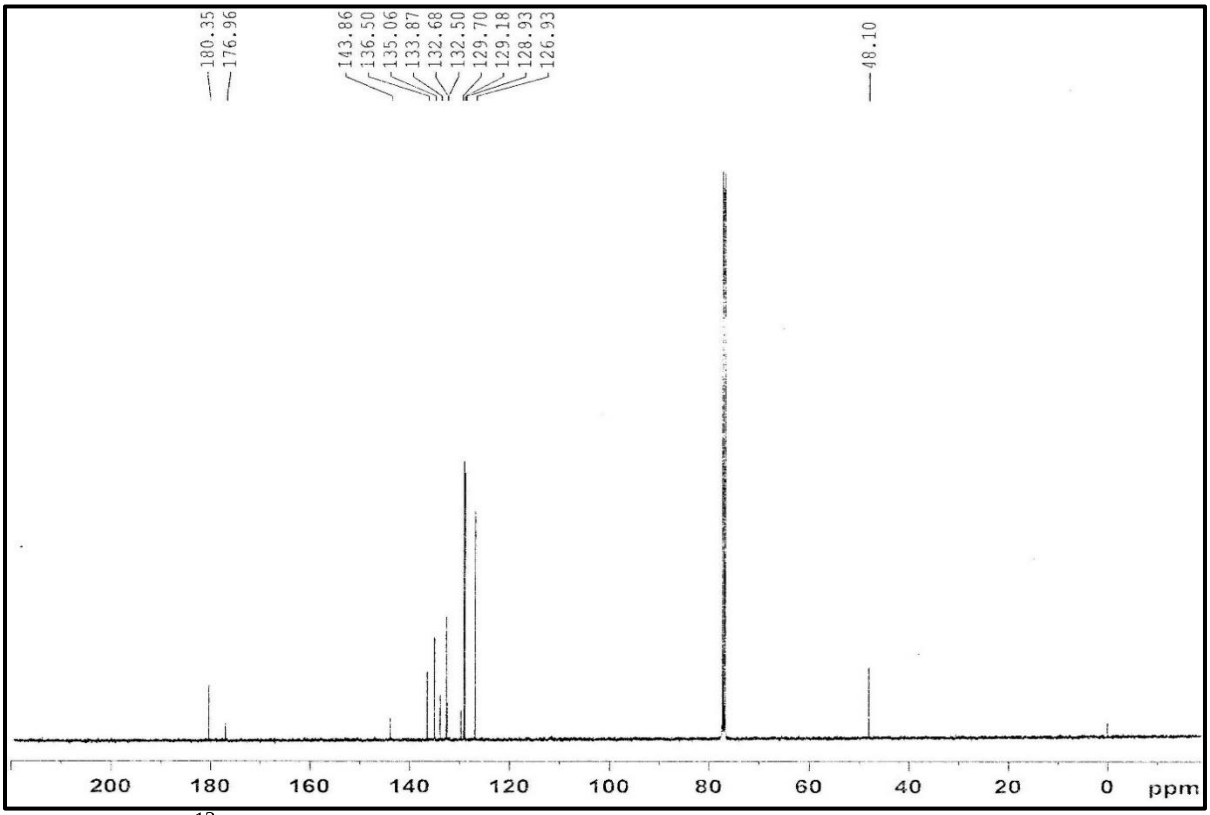

Annexure 14. ^{13}C NMR spectrum of 5.

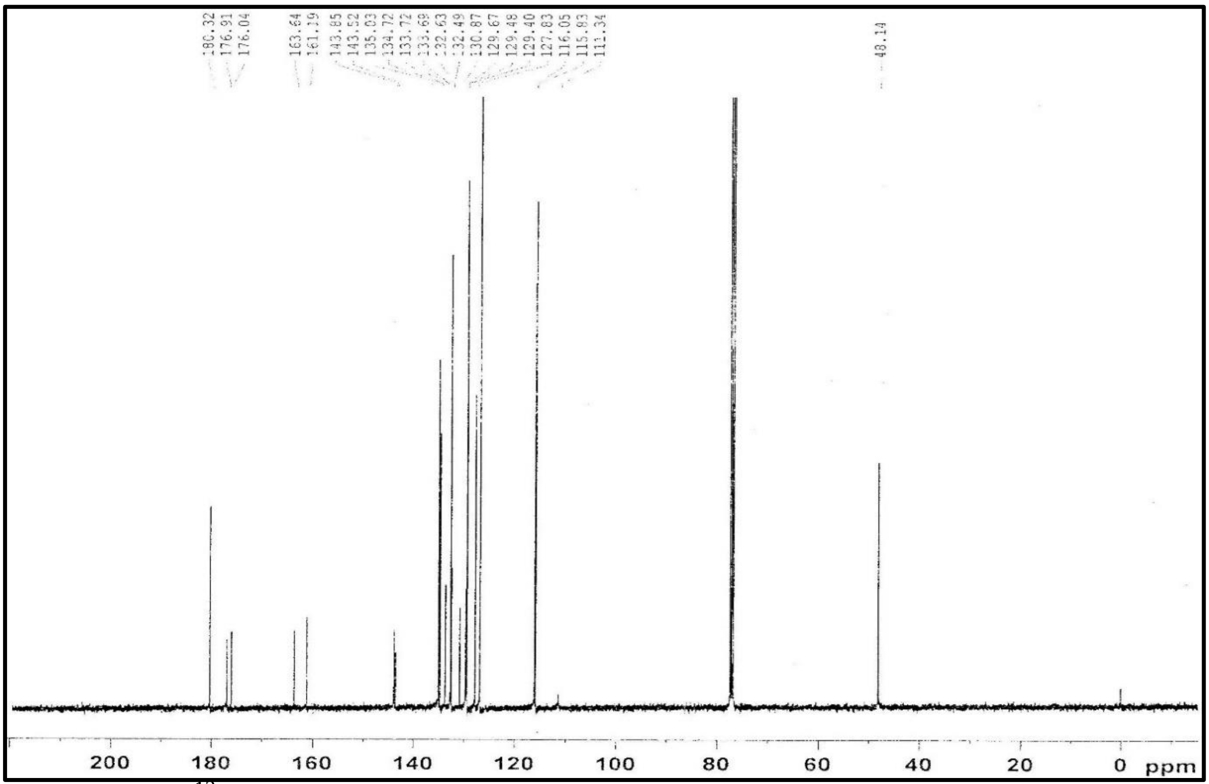

Annexure 15. ^{13}C NMR spectrum of 6.

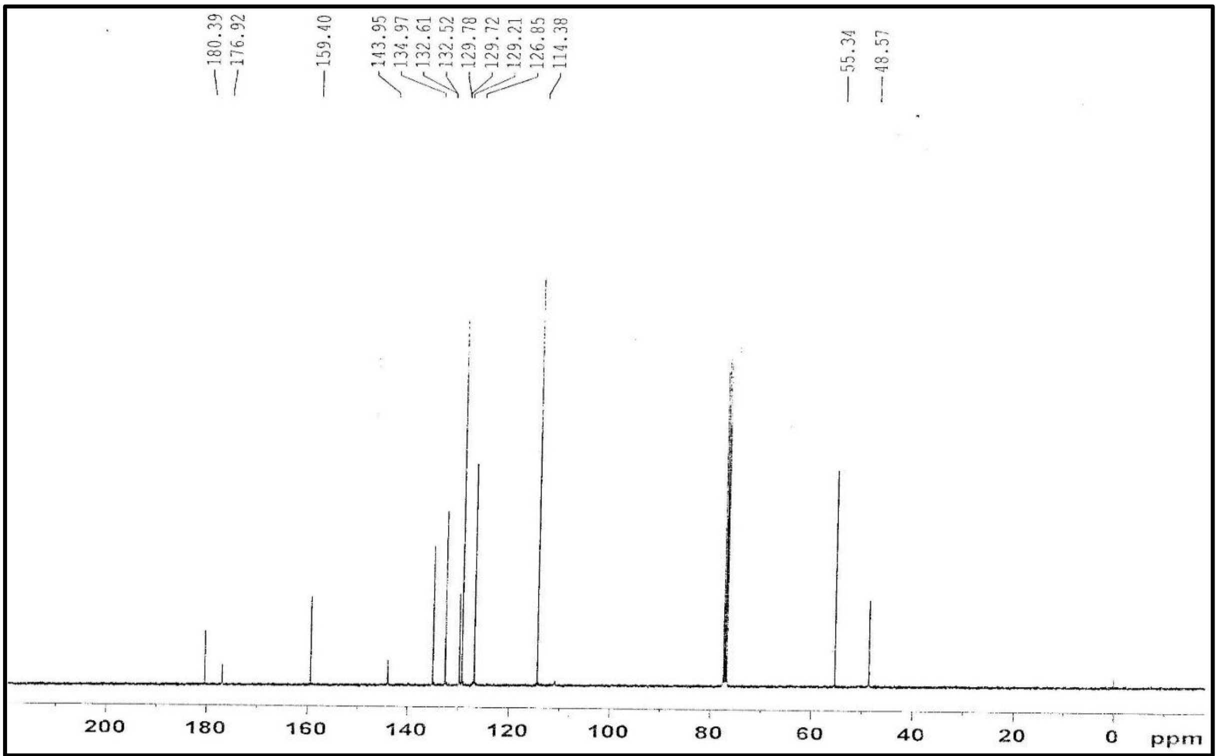

Annexure 16. ^{13}C NMR spectrum of 7.

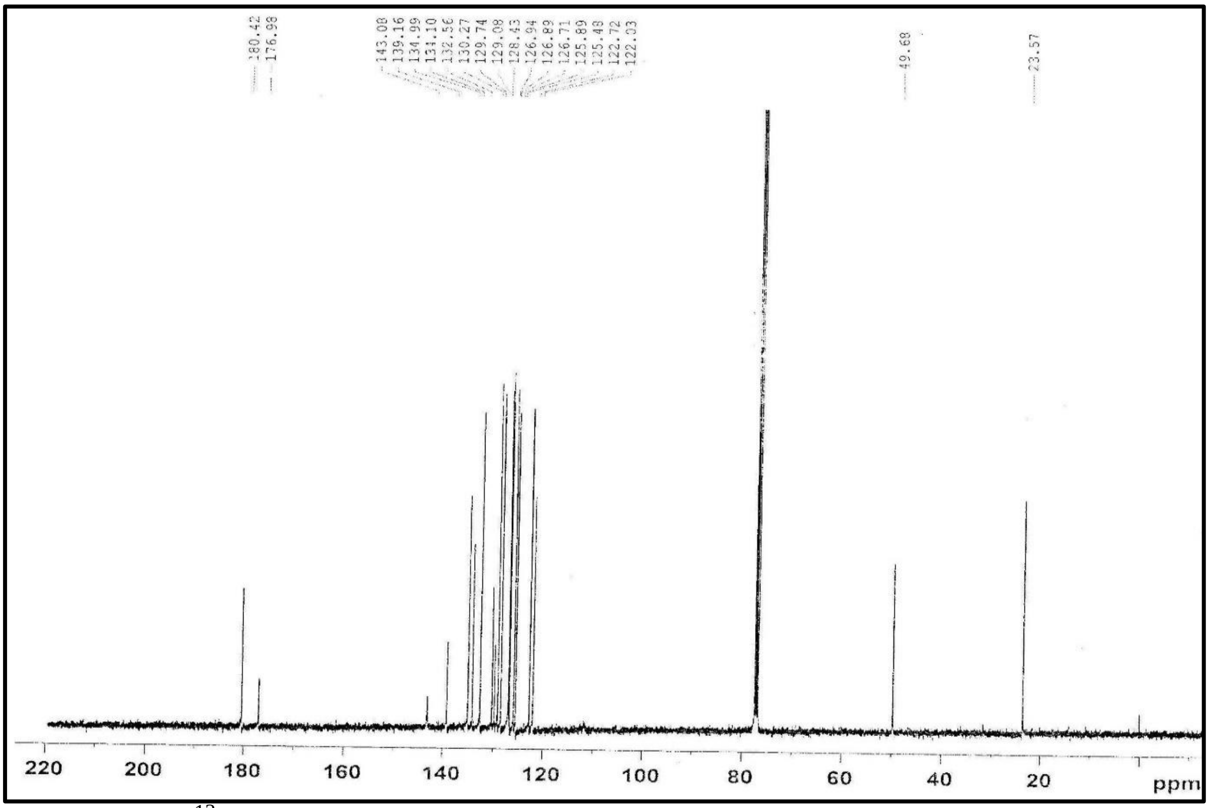

Annexure 17. ^{13}C NMR spectrum of **8**.

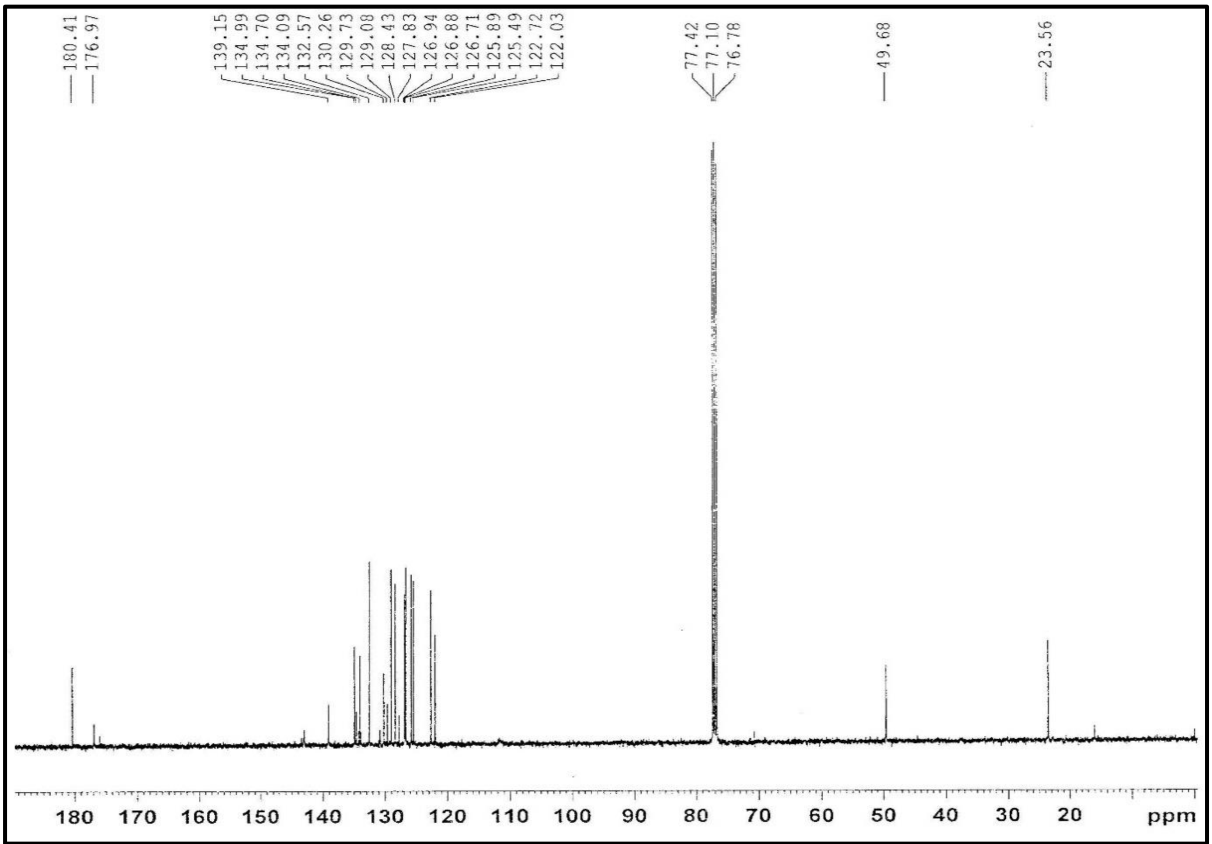

Annexure 18. ^{13}C NMR spectrum of **9**.

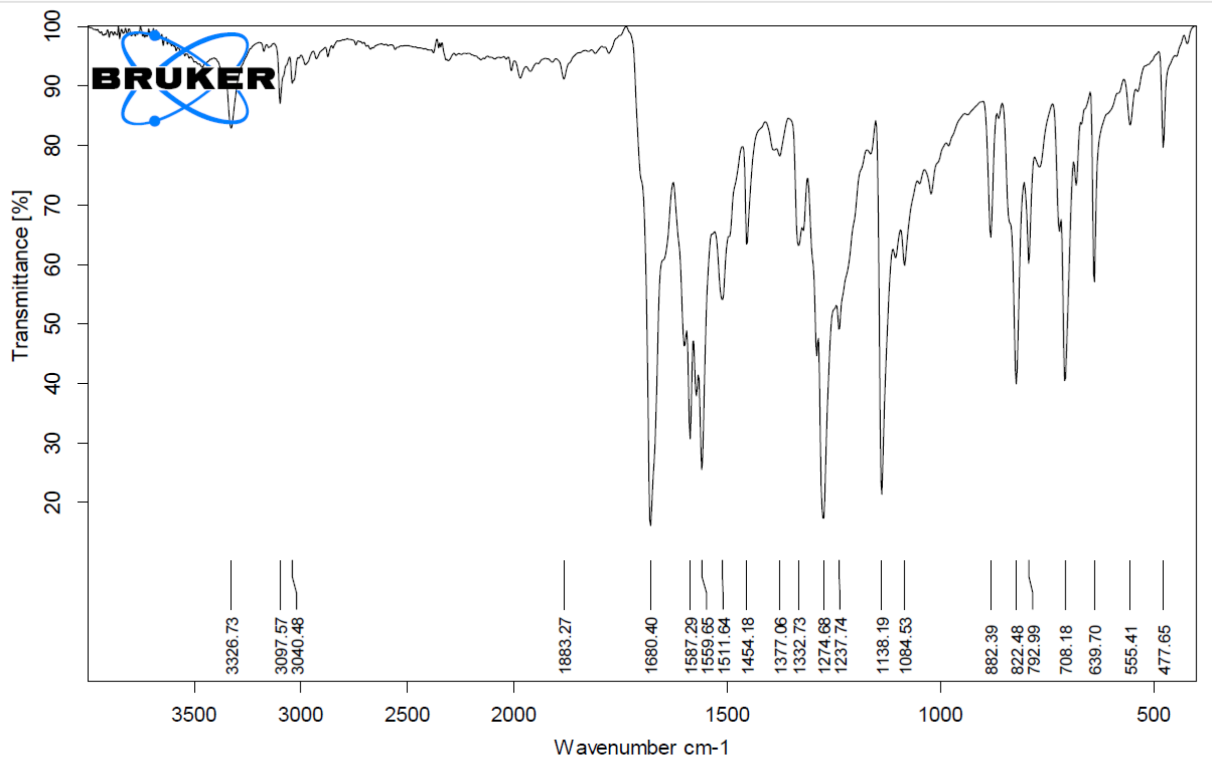

Annexure 19. IR spectrum of 1.

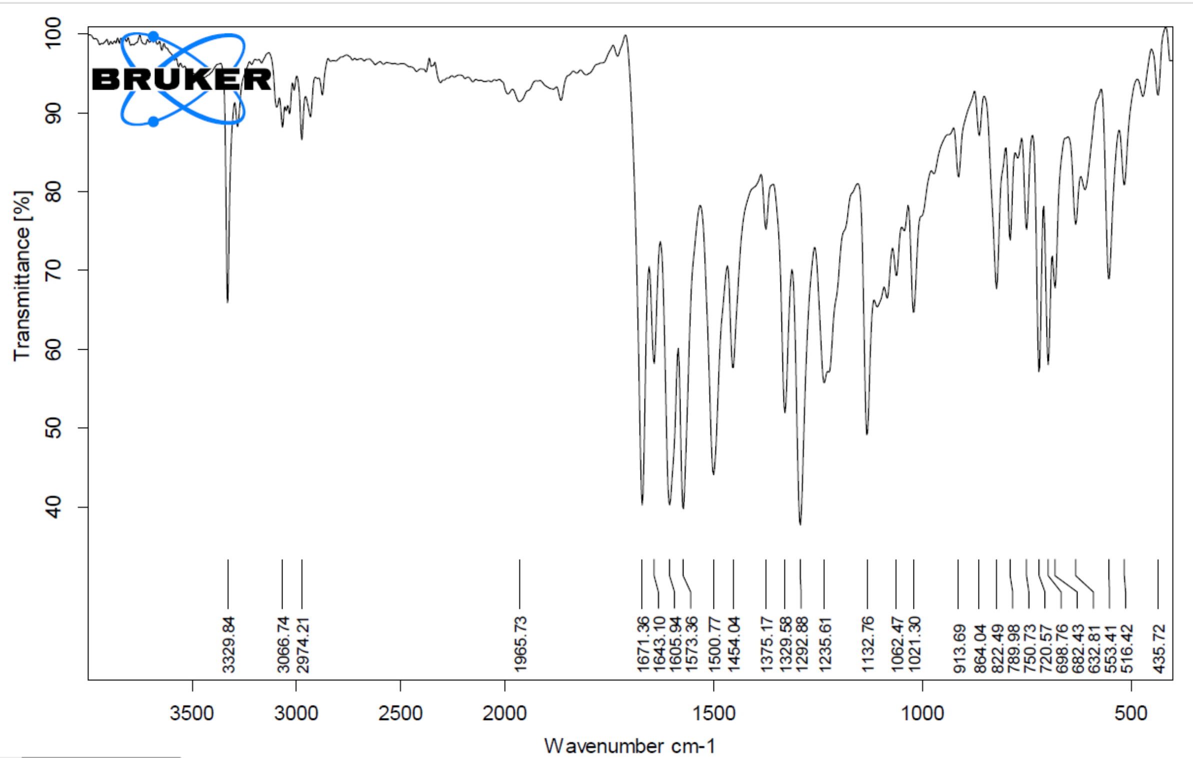

Annexure 20. IR spectrum of 2.

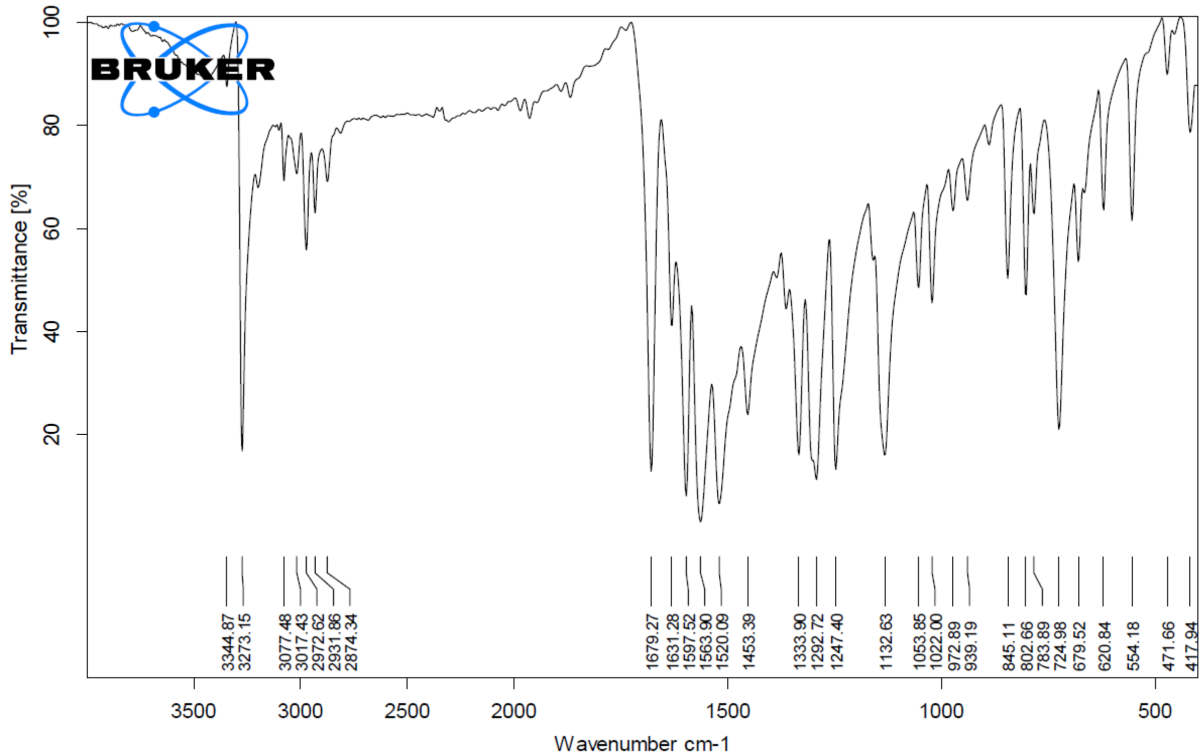

Annexure 21. IR spectrum of 3.

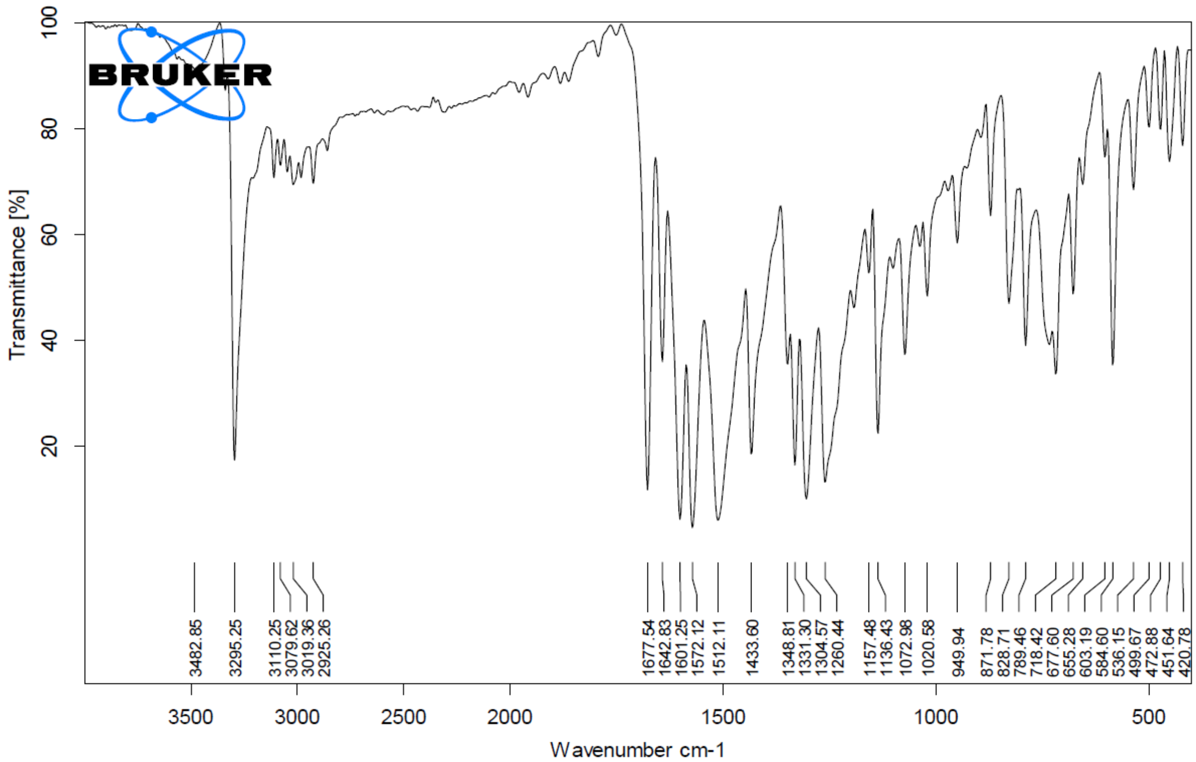

Annexure 22. IR spectrum of 4.

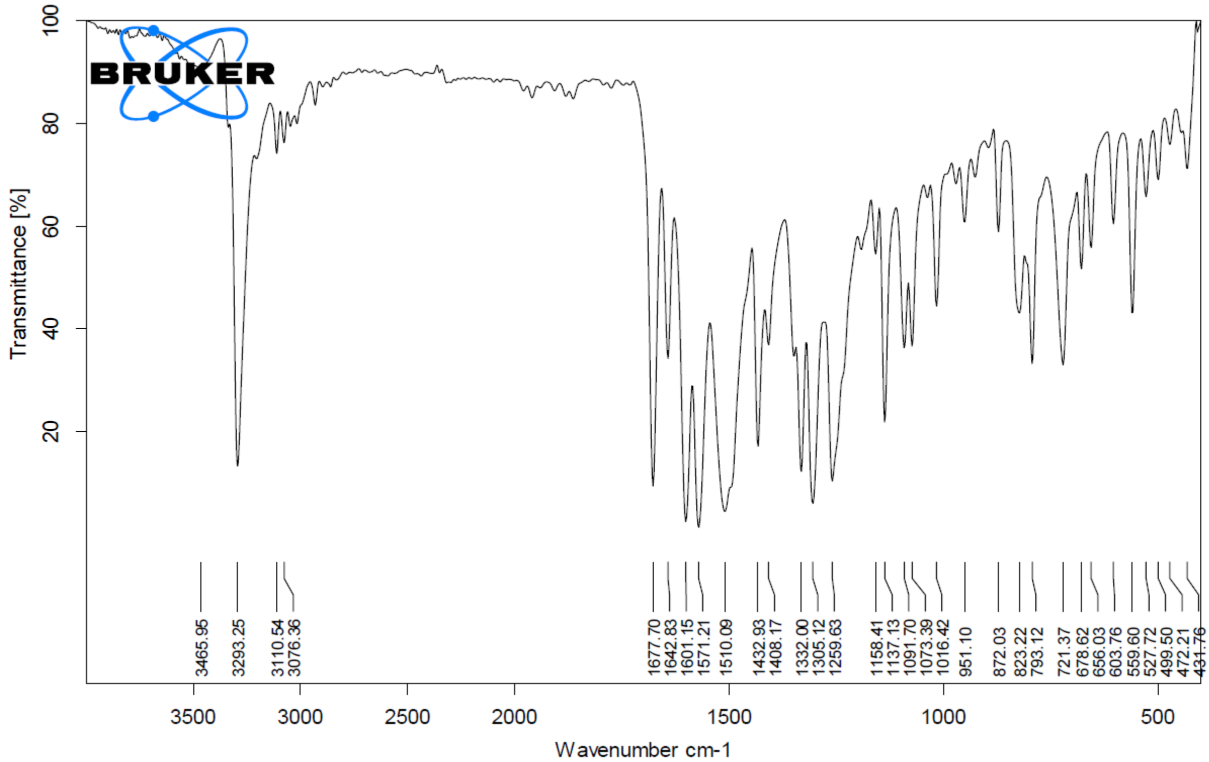

Annexure 23. IR spectrum of 5.

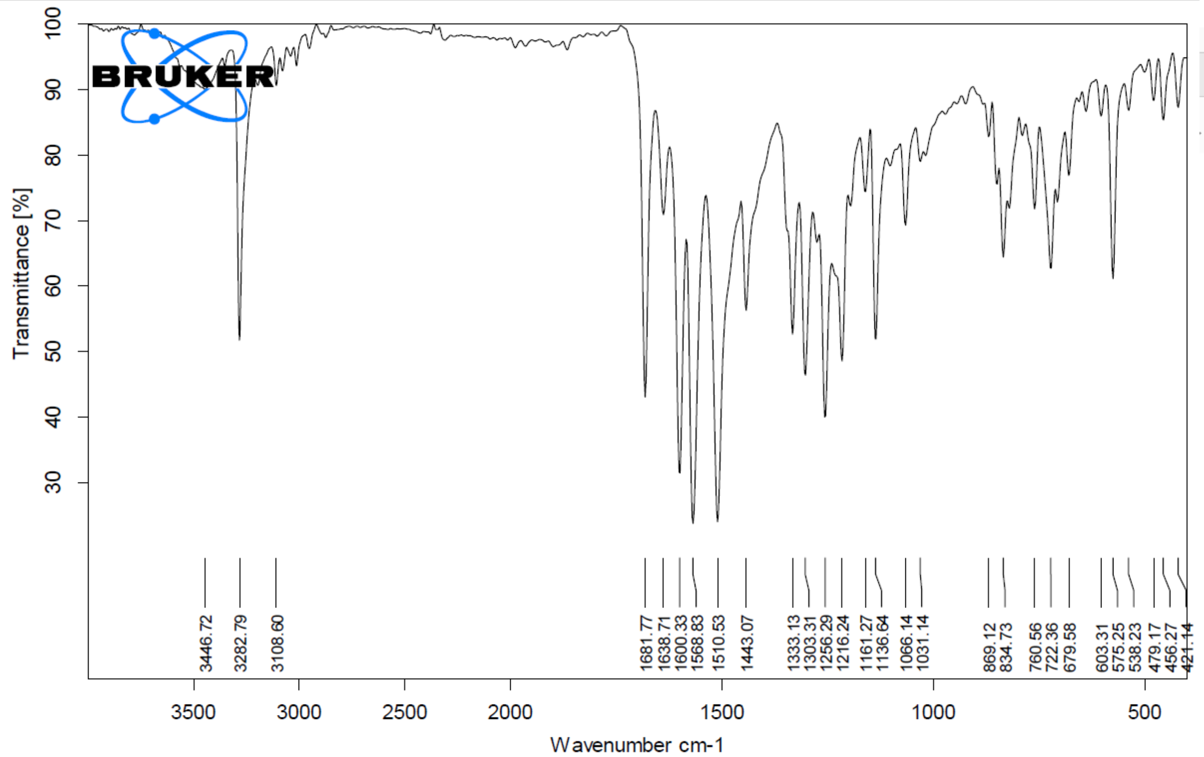

Annexure 24. IR spectrum of 6.

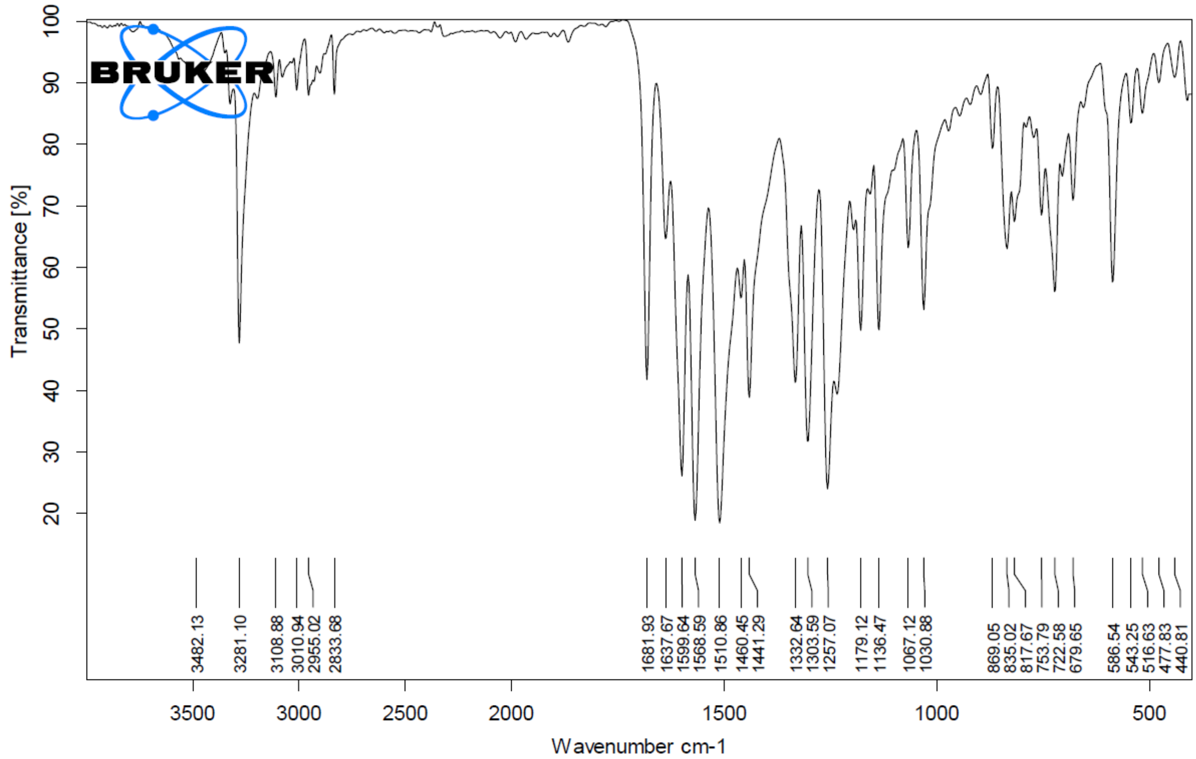

Annexure 25. IR spectrum of 7.

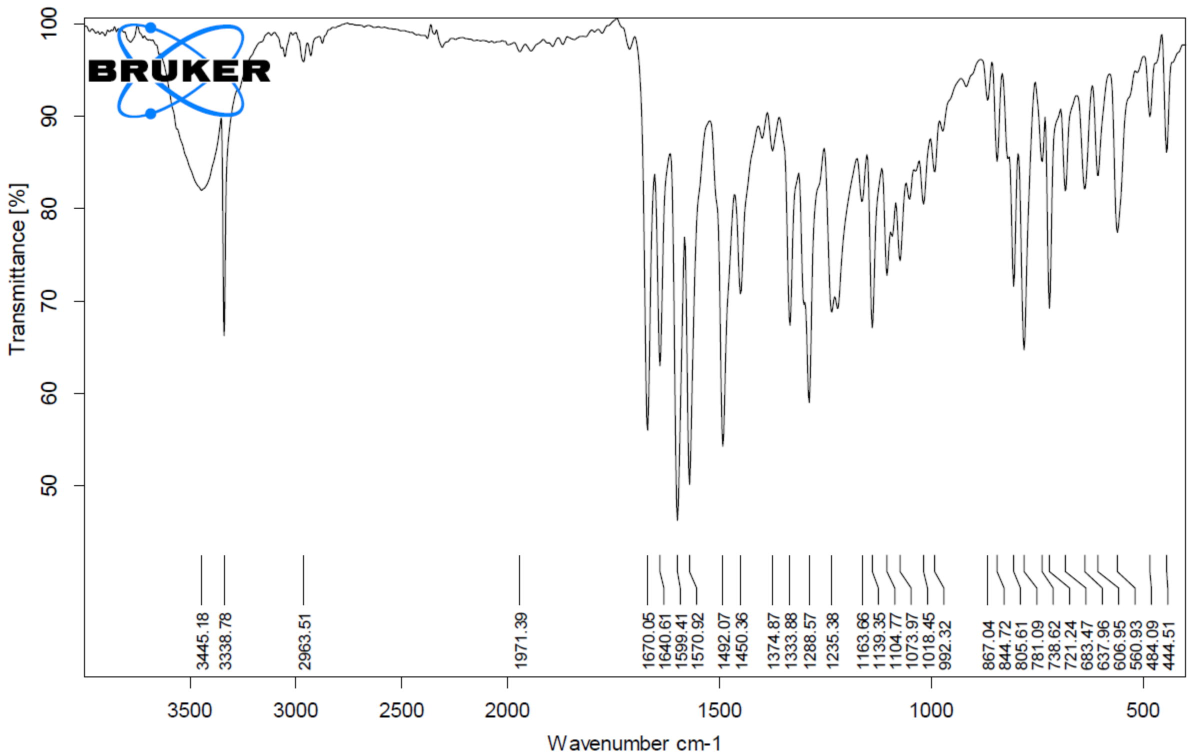

Annexure 26. IR spectrum of 8.

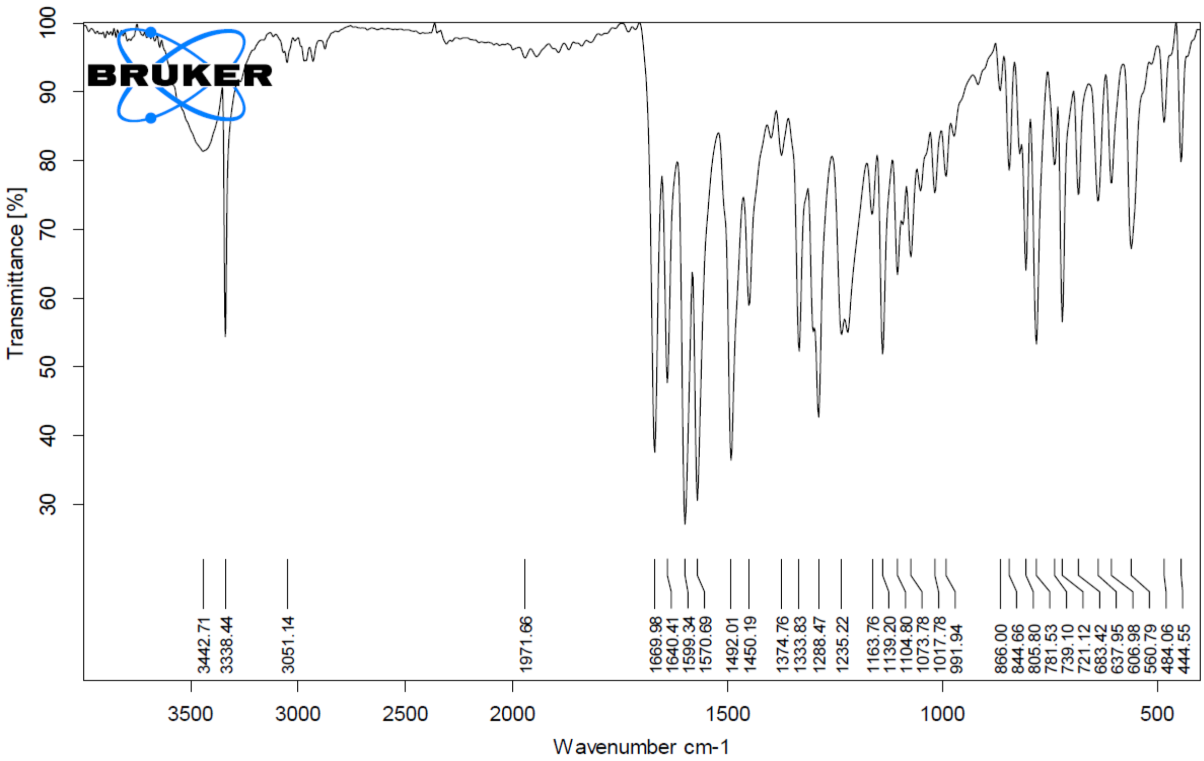

Annexure 27. IR spectrum of 9.